Multi-objective Optimization of Shell and Tube Heat Exchanger – a Case Study

Melkamu Embiale[a], Addisu Bekele[b,*], Chandraprabu Venkatachalam[b], Mohanram Parthiban[c]

[a]M.Sc. Mechanical Engineering Department, Adama Science and Technology University, Adama, Ethiopia
[b]Assistant Professor, Mechanical Engineering Department, Adama Science and Technology University, Adama, Ethiopia
[c]Lecturer, Mechanical Engineering Department, Adama Science and Technology University, Adama, Ethiopia

---***---

Abstract - *This paper presents design modification and optimization of an existing shell and tube heat exchanger of Awash Melkasa Aluminum Sulfate and Sulphuric Acid Share Company (AMASSA S.Co) which is the only sulphuric acid and aluminium sulphate producing factory in Ethiopia. The optimization is done by using univariate and ant colony optimization technique (ACO). Here multi-objective optimization of the heat transfer rate and cost of a shell and tube heat exchanger is presented with multiple Pareto-optimal solutions to capture the trade-off between the two objectives in both techniques. Five decision variables are considered: tube layout, tube diameter, fin height, fin space, and fin thickness. For these decision variables sensitivity analysis has been performed in order to observe the variational influences of decision variables over optimization objectives and then focus on more sensitive decision variables in a case of univariate technique to decrease problem complexities. In this study it is found that tube layout, fin height and fin space have more variational effect on objective variables. Finally Pareto front graphs are constructed for multi objective optimization and the best solution is selected by comparing the two techniques values based on requirements.*

Keywords: *Shell and tube heat exchanger; Multi-objective optimization; Ant Colony Optimization and Univariate Optimization*

1. INTRODUCTION

In heat exchangers, typical applications involve heating or cooling of a fluid stream of concern and evaporation or condensation of single or multicomponent fluid streams. In other applications, the objective may be to recover or reject heat, or sterilize, pasteurize, fractionate, distill, concentrate, crystallize, or control a process fluid. In a few heat exchangers, the fluids exchanging heat are in a direct contact. But in most heat exchangers, heat transfer between fluids takes place through a separating wall or separated by a heat transfer surface, for which shell and tube heat exchanger can be an example. Due to manufacturing and design flexibility, shell and tube heat exchangers are the most used heat transfer equipment in industrial processes. They are also easily adaptable to operational conditions. In this way, the design of shell and tube heat exchangers are very important subject in industrial processes. Nevertheless, some difficulties are found, especially in the shell-side design, because of the complex characteristics of heat transfer and pressure drop [1,2]. The shell and tube heat exchanger (STHE) under study for this paper is found in Awash Melkasa Aluminum Sulfate and Sulfuric Acid Share Company (AMASSA S.Co). Here the heat exchanger works in engineering principle's to extract heat of flue gas (SO_3) in order to make it 180 °C. For the STHE in Awash Melkasa Aluminum Sulfate and Sulfuric Acid Share Company the two system fluids in which heat is going to be exchanged is water and flue gas(SO_3). Flue gas with mass flow rate of 20 kg/s enters in to shell and exit with outlet temperature of 180 °C, whereas water at 80 °C enters the tube side and out at temperature of 130 °C. But the problems is that the tubes are damaged and water leaks from tube to the shell, as a result acid is formed in the shell. Having this information at hand, detail study of this heat exchanger and new geometry optimization will be run using general thermal equations for STHE heat transfer rate (heat load), pressure drop across the system and optimum total cost. The Geometry optimization is done by considering tube diameter, fin thickness, space, height and tube layout (Triangular or Rectangular Pattern). Finally the overall heat transfer rate, Pressure drop and cost are studied and the allowable design will be chosen from thermal design point of view.

* Corresponding Author

Email: addisu2009@gmail.com

2. METHODOLOGY

In this paper existing STHE will studied in detail and from which size of the shell and input and output temperature of fluids held constant as input parameter to size the modified STHE. Unknown parameters (decision variables) can be either dependent or independent variables. Then the whole STHE correlations are defined in terms of independent variables. For different independent variable variations, values of heat transfer rate and cost of STHE are different. In a case of optimization using Microsoft Excel, more influential independent variables on values of heat transfer rate and cost will considered in a specified ranges to decrease analysis complexity. But in MATLAB programing all independent variables will be considered. Finally, for each methods one best value will be selected in order to have satisfactory heat transfer rate and total cost. Of which, by compression one solution will take as a final modified STHE.

Detail process of the design methodology considerations are shown in figurer 2.1.

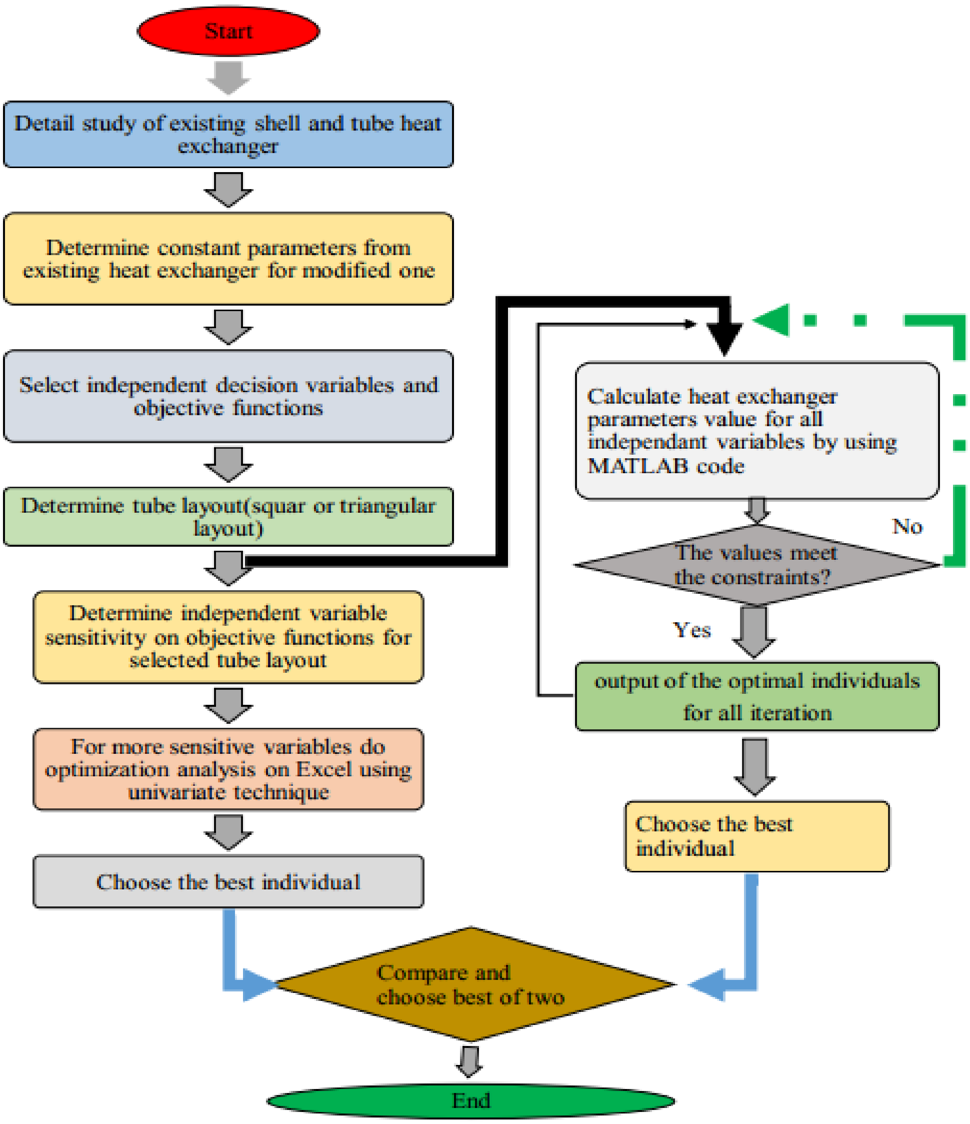

Figure 2. 1 Flow chart for the research work

3. HEAT EXCHANGER MODEL AND DESIGN FORMULATION

To analyse the exchanger heat transfer problem, a set of assumptions are introduced so that the resulting theoretical models are simple enough for the analysis. The following assumptions are made for the exchanger heat transfer problem formulations:

- The heat exchanger operates under steady-state conditions.
- Heat losses to or from the surroundings are negligible because it has 50 cm cotton insulation thickness.

- There are no thermal energy sources or sinks in the exchanger walls or fluids.
- The temperature of each fluid is uniform over every cross section in exchangers due to turbulence fluids are mixed enough.
- Wall thermal resistance is distributed uniformly in the entire exchanger.
- Phase changes in the fluid streams flowing through the exchanger is negligible.
- Longitudinal heat conduction in the fluids and in the wall is negligible.
- The fluid flow rate is uniformly distributed through the exchanger on each fluid side in each pass.

3.1 Design Formulation

Depending on input parameters heat transfer analysis of an exchanger can be performed by using any of the ε -NTU or LMTD methods. Therefore in this heat exchanger heat transfer analysis ε –NTU method is used.

In the ε -NTU method, the heat transfer rate from the hot fluid to the cold fluid in the exchanger is expressed as

$$\dot{Q} = \varepsilon C_{min}\left(T_{h,in} - T_{c,in}\right) = \varepsilon C_{min}\Delta T_{max} \tag{3.1}$$

ε, can be determined directly from the operating temperatures and heat capacity rates [3].

$$\varepsilon = \frac{C_c\left(T_{c,out} - T_{c,in}\right)}{C_{min}\left(T_{h,in} - T_{c,in}\right)} = \frac{C_h\left(T_{h,in} - T_{h,out}\right)}{C_{min}\left(T_{h,in} - T_{c,in}\right)} \tag{3.2}$$

Where ε is the heat exchanger effectiveness, sometimes referred to as the thermal efficiency, C_{min} is the minimum of C_c and C_h; ΔT_{max}=$\left(T_{h,in} - T_{c,in}\right)$ is the fluid inlet temperature difference (ITD).

Heat Capacity Rate Ratio C* is simply a ratio of the smaller to larger heat capacity rate for the two fluid streams.

$$C^* = \frac{C_{min}}{C_{max}} = \frac{\left(\dot{m}C_p\right)_{min}}{\left(\dot{m}C_p\right)_{max}} \tag{3.3}$$

Number of Transfer Units NTU

The number of transfer units NTU is defined as a ratio of the overall thermal conductance to the smaller heat capacity rate [3]:

$$NTU = \frac{UA}{C_{min}} \tag{3.4}$$

In general heat exchanger effectiveness is dependent on the number of transfer units NTU, the heat capacity rate ratio C*, and the flow arrangement for a direct-transfer type heat exchanger. Therefore for shell and tube, one shell pass (2, 4 . . . tube passes) arrangement heat exchanger effectiveness is represented as:

$$\varepsilon = 2\left\{1 + C^* + (1 + C^{*2})^{1/2} \times \frac{1 + \exp[-(NTU)(1 + C^{*2})^{1/2}]}{1 - \exp[-(NTU)(1 + C^{*2})^{1/2}]}\right\}^{-1} \tag{3.5}$$

3.2. Overall Heat Transfer Coefficient

The equation basically sums up all the resistances encountered during the heat transfer and taking the reciprocal gives us the overall heat transfer coefficient [4].

$$U = \frac{1}{AR_{tot}} \tag{3.6}$$

$$R_{tot} = R_s + R_{f,s} + R_w + R_{f,t} + R_t \tag{3.7}$$

Convection resistances R_t and R_s are calculated from the definition of convection resistance

$$R_{conv} = \frac{1}{hA} \tag{3.8}$$

for in case of a tube of length L_1 and inner and outer diameters of Di and Do , from

$$R_w = \frac{\ln\frac{D_o}{D_i}}{2\pi k_w L_1} \qquad (3.9)$$

Typical values of fouling resistance per surface area $R_f^{"}$ (m^2K / W) for the type fluid and the fouling layer resistance then obtained from [5]

$$R_f = \frac{R_f^{"}}{A} \qquad (3.10)$$

From the above thermal resistance equations the value of U can be obtained.

$$U = \left(\frac{A}{A_i h_i} + \frac{\dot{R}_{fDi} A}{A_i} + \frac{\dot{R}_{fDo}}{\eta_w} + \frac{1}{h_o \eta_w} + AR_w\right)^{-1} \qquad (3.11)$$

Wall resistance for N_t circular tubes with a multiple-layer wall can be given by equation:

$$R_w = \frac{1}{2\pi L_1 N_t}\left(\sum_j \frac{\ln(D_{j+1}/D_j)}{k_{w,j}}\right) \qquad (3.12)$$

Where k_w= wall thermal conductivity, D_j and D_{j+1} = consecutive diameters between a layer and j = number of tube layers.

3.3. Fin Efficiency

Fins are generally used on the outside, but they may be used on the inside of the tubes in some applications. They are attached to the tubes by a tight mechanical fit, adhesive bonding, welding, or extrusion [6].

A logical definition of fin efficiency is therefore

$$\eta_f = \frac{\dot{Q}_f}{\dot{Q}_{max}} = \frac{\dot{Q}_f}{hA_f\,\theta_b} \qquad (3.13)$$

$$\eta_f = \frac{\tanh(m\psi)}{m\psi} \qquad (3.14)$$

$$m = \left(\frac{2h_o}{k\tau}\right)^{0.5} \qquad (3.15)$$

$$\psi = \left(\frac{D_f + \tau - D_r}{2}\right)\left(1 + 0.35\ln\left(\frac{D_f + \tau}{D_r}\right)\right) \qquad (3.16)$$

where A_f is the surface area of the fin.

In contrast to the fin efficiency η_f, which characterizes the performance of a single fin, the overall surface efficiency η_w characterizes an array of fins and the base surface to which they are attached.

$$\eta_w = \frac{\dot{Q}_t}{\dot{Q}_{max}} = \frac{\dot{Q}_t}{hA\,\theta_b} \qquad (3.17)$$

$$A_f = L_1 N_t N_f\left[2\pi\left(\frac{{D_f}^2 - {D_r}^2}{4}\right) + \pi D_f \tau\right] \qquad (3.18)$$

$$A_b = \pi D_r(L_1 N_t - L_1 N_t N_f \tau) \qquad (3.19)$$

$$A = A_f + A_b \qquad (3.20)$$

$$A_i = \pi D_i N_t L_1 \qquad (3.21)$$

$$\eta_w = \frac{A_b + \eta_f A_f}{A} \quad (3.22)$$

Where $\dot{Q}_t$ is the total heat rate from the surface area A associated with both the fins and the exposed portion of the base (often termed the prime surface). If there are N_f fins in the array, each of surface area A, and the area of the prime surface is designated as A_b, the total surface area is

$$A = N_f A_f + A_b \quad (3.23)$$

The maximum possible heat rate would result if the entire fin surface, as well as the exposed base, were maintained at T_b. The total rate of heat transfer by convection from the fins and the prime (unfinned) surface may be expressed as.

$$\dot{Q}_t = N_t \eta_f A_f h\,\theta_b + hA_b\,\theta_b \quad (3.24)$$

Where the convection coefficient this assumed to be equivalent for the finned and prime surfaces [7].

Hence $$\eta_w = 1 - \frac{N_f A_f}{A}(1 - \eta_f) \quad (3.25)$$

3.4. Convective Heat Transfer Coefficient on Shell Side

The flow of gases over banks of finned tubes has been extensively studied and numerous correlations for this geometry are available in the open literature. Among these, the correlation of Briggs and Young has been widely used [8]:

$$N_{us} = 0.134 R_{es}^{0.681} P_{rs}^{1/3} \left(l/b\right)^{0.2} \left(l/\tau\right)^{0.1134} \quad (3.26)$$

Where:

$$Nu_s = h_o D_r / k_s$$

$$R_{es} = D_r V_{max} \rho_s / \mu_s$$

The Reynolds number is based on the tube outside diameter and the velocity on the cross flow area of the shell. V_{max}= maximum air velocity in tube bank, D_r=root diameter, l = fin spacing, b = fin height, τ = fin thickness, k_s = thermal conductivity of gas, ρ_s = density of gas, μ_s = viscosity of gas, h_o = gas-side heat-transfer coefficient

The fin spacing is related to the number,N_f, of fins per unit length by the following equation:

$$l = 1/N_f - \tau \quad (3.27)$$

For an inline tube arrangement:

$$V_{max} = \frac{L_1 L_3 V_{face}}{\left[(X_t - D_r)L_1 - (D_f - D_r)\tau N_f L_1\right]\frac{L_3}{X_t}} \quad (3.28)$$

For the staggered tube arrangement:

$$V_{max} = \frac{L_1 L_3 V_{face}}{\left[\left(\frac{L_3}{X_t} - 1\right)\left[(X_t - D_r) - (D_f - D_r)\tau N_f\right] + (X_t - D_r) - (D_f - D_r)\tau N_f\right] L_1} \quad (3.29)$$

$$V_{face} = \frac{\dot{m}}{\rho_s A_{face}}$$

Where: V_{face} is face velocity the average air velocity approaching the first row of tubes, X_t=pitch in the transverse, X_L=pitch in the longitudinal tube row, L_1=tube length, L_3=the no flow dimension length.

3.5. Convective Heat Transfer Coefficient on Tube Side

Heat transfer to fluids flowing inside pipes and ducts is a subject of great practical importance. And the correlations presented below are adequate to handle the vast majority of process heat-transfer applications [8].

For heat-transfer coefficient, hi, the Seider–Tate and Hausen equations are used as follows.

For $R_{et} \geq 10^4$,

$$\mathrm{Nu_t} = 0.023\mathrm{R_{et}^{0.8}P_{rt}^{1/3}}\,(\mu_t/\mu_w)^{0.14} \tag{3.30}$$

For $2100 < R_{et} < 10^4$

$$\mathrm{Nu_t} = 0.116\left[R_{et}{}^{2/3} - 125\right]\mathrm{P_{rt}^{1/3}}(\mu_t/\mu_w)^{0.14}\left(1 + \frac{D_i}{L_1}^{2/3}\right) \tag{3.31}$$

For $R_{et} \leq 2100$,

$$\mathrm{Nu_t} = 1.86\left(R_{et}\mathrm{P_{rt}}\frac{D_i}{L_1}\right)^{1/3}(\mu_t/\mu_w)^{0.14} \tag{3.32}$$

Where

$\mathrm{Nu_t}$ = Nusselt Number $\equiv \mathrm{h_iD_i}/\mathrm{k}_t$

$\mathrm{R_{et}}$ = Reynolds Number $\equiv \mathrm{D_i}V_t\rho_t/\mu_t$

$V_t = \frac{4\dot{m}_t(n_p/n_t)}{\rho_t\pi D_i^2}$, $\dot{m}_t$= total mass flow rate of tube-side fluid, n_p = number of tube-side passes, N_t= number of tubes, $P_{rt} \equiv$ Prandtl Number $\equiv C_{pt}\mu_t/k_t$, D_i = inside pipe diameter, V_t = average fluid velocity, $(\mu/\mu_w)^{0.14}$ = viscosity correction factor (dimensionless). But the value of $(\mu/\mu_w)^{0.14}$ is approaches to 1, due to this mostly it is neglected and C_{pt}, μ_t, ρ_t, k_t = fluid properties evaluated at the average bulk fluid temperature.

3.6. Pressure Drop on Shell Side

The pressure drop for flow across a bank of tubes is given by the following equation:

$$\Delta P_{fs} = \frac{2f_s N_r G^2{}_s}{\rho_s} \tag{3.33}$$

Where: f_s = Fanning friction factor, N_r = number of tube rows, $G_s = V_{max}\rho$, $R_{esp} = D_h V_{max}\rho_s/\mu_s$, $D_h = \frac{4A_oL_2}{A}$, L_2=the core length for flow normal to the tube bank and A_o= minimum free-flow area.

For an inline tube arrangement:

$$A_o = [(X_t - D_r)L_1 - (D_f - D_r)\tau N_f L_1]\frac{L_3}{X_t} \tag{3.34}$$

For the staggered tube arrangement:

$$A_o = \left[\left(\frac{L_3}{X_t} - 1\right)[(X_t - D_r) - (D_f - D_r)\tau N_f] + (X_t - D_r) - (D_f - D_r)\tau N_f\right]L_1 \tag{3.35}$$

A=total heat transfer area both for fine and prime surface.

$A = A_b + A_f$

$$A_b = \pi D_r(L_1 N_T - N_f L_1 N_T \tau) \tag{3.36}$$

$$A_f = \left[2\pi\left(\frac{D_f{}^2 - D_r{}^2}{4}\right) + \pi D_f \tau\right]N_f L_1 N_t \tag{3.37}$$

For an inline tube arrangement:

$$N_t = \frac{L_2 L_3}{X_t X_l}$$

For the staggered tube arrangement:

$$N_t = \frac{L_3}{X_t}\frac{L_2/X_l + 1}{2} + \left(\frac{L_3}{X_t} - 1\right)\frac{L_2/X_l - 1}{2} \tag{3.38}$$

$$f_s = \left\{1 + \frac{2e^{-(a/4)}}{1+a}\right\}\left\{0.012 + \frac{27.2}{R_{e_{eff}}} + \frac{0.29}{{R_{es}}^{0.2}{}_{eff}}\right\} \tag{3.39}$$

Where: $a = {}^{(P_T - D_f)}/_{D_r}$, $R_{e_{eff}} = R_e({}^{l}/_{b})$ and $D_f = D_r + 2b = \text{fin OD}$

In addition to the tube bank, there are other sources of friction loss on the gas side. Although the friction loss due to each of those factors is usually small compared with the pressure loss in the tube bank, in aggregate the losses often amount to between 10% and 25% of the bundle pressure drop [3, 8].

3.7. Pressure Drop on Tube Side

The pressure drop due to fluid friction in the tubes with the length of the flow path set to the tube length times the number of tube passes. Thus,

$$\Delta P_{ft} = \frac{f_t N_t L_1 {G^2}_t}{2000 D_i s \Phi} \tag{3.40}$$

Where: ΔP_{ft}= pressure drop (Pa), f_t = Darcy friction factor (dimensionless), L_1 = tube length (m), G_t = mass flux (kg /s · m^2), s = $\frac{\rho_t}{\rho_w}$ fluid specific gravity (dimensionless), Φ = viscosity correction factor (dimensionless) =$({}^{\mu_s}/_{\mu_w})^{0.14}$ and for turbulent flow = $({}^{\mu_s}/_{\mu_w})^{0.25}$ for laminar flow. But the value of Φ is approaches to 1 due to this mostly it is neglected.

The minor losses on the tube side are estimated using the following equation:

$$\Delta P_{rt} = 5 \times 10^{-4}(2n_p - 1.5)\,{}^{{G^2}_t}/_{s} \tag{3.41}$$

For turbulent flow in commercial heat-exchanger tubes, the following equation can be used for $R_{et} \geq 3000$:

$$f_t = 0.4137 {R_{et}}^{-0.2585} \tag{3.42}$$

For $R_{et} \leq 3000$, laminar flow the friction factor is given by:

$$f_t = \frac{64}{R_{et}} \tag{3.43}$$

3.8. Cost Estimation

Cost is always an important consideration in designing any process equipment. In heat exchanger cost can be broken into two principal components – capital or investment cost and operating cost.

The capital cost for heat exchangers increases with increase in the heat transfer area whereas operating cost is primarily pumping cost. The pumps must provide work to overcome the pressure drop on the tube side and that on the shell side.

The operating cost C_{op} and the initial investment C_{in} for the shell and the tube can be approximated as follows.

$$C_T = C_{in} + C_{op} \tag{3.44}$$

$$C_{in} = F_p F_m F_l C_B \tag{3.45}$$

Where, F_p, F_m, C_B, F_l are pressure factor, material factor, tube length factor and types of heat exchanger respectively.

For carbon steel shell and steel tube materials

$F_m = a + (\frac{A}{100})^b$, a=1.55, b=0.05

Pressure factor F_p=0.9876, $F_l = 1.25$ for length 2.44 m.

$C_B = exp(11.667 - 0.809[ln(A/0.093)] + 0.009005[ln(A/0.093)]^2)$, A is in m²

$$C_{op} = \sum_{k=1}^{n_y} \frac{C_o}{(1+i)^k} \tag{3.46}$$

Where C_o is the annual cost, n_y lifetime, and i is the annual inflation rate.

The total operating cost is dependent on the pumping power to overcome the pressure drop from both shell and tube side flow [9].

$$C_o = P \times kel \times H \tag{3.47}$$

$$P = \frac{1}{\eta}\left(\frac{\dot{m}_s \Delta P_{sfT}}{\rho_s} + \frac{\dot{m}_t \Delta P_{tT}}{\rho_t}\right) \tag{3.48}$$

Where kel the unit price of electrical energy, P is pumping power; H is the hours of operation per year and η is the pumping efficiency.

Table 3. 1 Existing (original) heat exchanger parameter values

Parameter name	Shell side (SO_3) at average temperature	Tube side (Water) at average temperature
Root diameter D_r(m)	-	0.075
Inside diameter D_i(m)	-	0.04
Fin spacing ℓ(m)	-	0.023
Fin height b(m)	-	0.02
Fin thickness τ(m)	-	0.007
Number of fins per leng. N_f	-	74
Number of tube passes n_p	-	2
Number of tubes N_t	-	64
Thermal conductivity k(W/m. K)	0.03747	0.682
Density ρ(kg/m^3)	0.757	954.575
Viscosity μ(kg/(m. s))	2.5787×10^{-5}	2.67×10^{-4}
Prandtl number (P_r)	0.705	1.67
Pitch diameter P_T(m)	-	0.13
Fin diameter D_f(m)	-	0.115
Tube length L_1(m)	-	2.2
Pipe thickness	-	0.012
Mass flowrate $\dot{m}(^{kg}/_s)$	20	2.435
T(°C) inlet and outlet respectively	205.04, 180	80, 130
Heat transfer coefficient h($W/m^2.k$)	227	682.05
Fin efficiency η_f(%)	_	77.048
Overall efficiency η_w(%)	_	83.1856
Pressure drop $\Delta P(kPa)$	12209	149.74
Heat transfer rate $\dot{Q}$(W)	5.133×10^5	

To select the best values to fulfil the objective functions, total cost evaluation has to be required. Functional years of original (existing) STHE (n_y) = 20 years, annual discount rate (i) = 10 %, unit price of electrical energy in Ethiopia (Kel) = 0.06 $\$/kWh$, Pump efficiency $\eta = 75\ \%$ *and* the hours of operation per year(H) = 8040 h/year (The remaining days being nominal maintenance shutdown days).

From which total cost of original heat exchanger (CT) =1.8294× 10^6 \$.

4.9. Selection of Decision Variables

Existing shell and tube heat exchanger has been studied above in detail. Standing from which the modified design STHE will be studied.

Impute data used in modified STHE is: Inlet and outlet temperature and mass flowrate of both fluids along with their physical properties, tube length, tube thickness, and length, width and height of the shell. Which is taken from the existing STHE because this heat exchanger is erected with in one frame with evaporator and erecting it alone and changing the shape is leading to another cost.

Here, the total cost and the heat transfer rate are the two objective functions. To fulfil the two needed objective functions optimization problem should be required.

Optimization problem is exactly that, a problem for which the one want to select the best possible, optimal, solution from a set of alternatives.

The main objective of this optimization is to find out the minimum value for the total cost and maximum heat transfer rate of the heat exchanger simultaneously.

The existing shell and tube heat exchanger study was rating problem that stands from design parameters and some operating conditions with those unknown values operating parameters were calculated. But modified design will be opposite of this that is sizing problem.

Objective functions subjected to constraint taken from existing STHE heat transfer rate and total cost:

$\dot{Q} \geq 5.133 \times 10^5$ W and CT $\leq 1.8294 \times 10^6$ \$

In modification, shell size is not considered because it is inter locked with evaporator and leads to additional cost.

So that modified STHE design decision variable parameters are reduced to:

- ✓ Tube diameter (D_i)
- ✓ Fin spacing (ℓ)
- ✓ Fin height (b)
- ✓ Fin thickness (τ)
- ✓ Tube layout (triangular and square)
- ✓ Number of tubes(N_t)
- ✓ Number of rows(N_r)
- ✓ Number of passes(n_p)
- ✓ Pitch length(P_T)
- ✓ Number of fin(N_f)

The variables listed above are both dependent and independent variables. The last five are dependent whereas the first five are independent variables. Since dependent variables can be expressed with independent values, it doesn't need to change the values of dependent variables rather it can be varies whenever changing independent variables.

Due to these decision variables are decreased to five variables: fin space, fin height, tube diameter, Tube layout and fin thickness.

From variables listed above, tube layout (square and triangular) effects with the same parameter values are listed in table 3.2.

Table 3.2 Comparison between square and triangular tube layouts

Tube layout	N_T	n_p	A	h_i	h_o	U	ε	$\dot{Q}$	N_r	ΔP_{fst}	ΔP_{tT}
Square (Existing)	64	2	94.54	682.05	227	62.8	0.39	513300	16	12209	149.74
Triangular (modified)	70	2	102.08	4207.6	221.86	103.37	0.54	715519.6	20	13857.22	146.22

U, h_i and h_o are expressed in (W/m^2k) and $\dot{Q}$ (W), $\Delta P_{fst}(Pa)$, $\Delta P_{tT}(Pa)$ and $A(m^2)$

Here the table values were calculated from the same impute parameters that is fluids temperature, mass flow rate, tube length, tube diameter, tube thickness, number of fin, fin length, fin space, fin height and shell length, width and height. These results tells that number of tubes and rows increase due to compactness of the tube in triangular tube layout. Heat transfer area which is direct related to capital cost of STHE increases by 7.39 % whereas heat transfer coefficients in the tube and shell decreases because of decrease of Reynolds number. But overall heat transfer coefficient improved by 64.6 %. Heat transfer rate and performance of heat exchanger are raised by 39.4 and 37.17 % respectively with 13.5 % shell pressure drop penalty and 2.35 % tube pressure drop benefit.

Finally, conclusion can be drawn that triangular tube layout can be a good choice for modified shell and tube heat exchanger design if its parameters are adjusted in optimized way.

3.10. Sensitivity Analysis

Sensitivity analysis can be performed in order to observe the variation influences of design parameters over optimization objectives. Virational effects of four decision variables on the problem objectives of heat transfer rates and total cost of heat exchanger is shown below in Figure 3.1 to 3.4. Best solutions will be selected by influences of decision variables over problem objectives. The remaining variables stays constant during evaluations. Decision variables and their range of variation are listed in Table 3.3.

Table 3.3 Decision variables and their range

Decision variables	**Range(m)**
Tube diameter (D_i)	0.034, 0.036, 0.038, **0.04**, 0.042, 0.044, 0.046
Fin spacing (ℓ)	0.017, 0.019, 0.021, **0.023**, 0.025, 0.027, 0.029
Fin height (b)	0.014, 0.016, 0.018, **0.02**, 0.022, 0.024, 0.026
Fin thickness (τ)	0.013, 0.011, 0.009, **0.007**, 0.005, 0.003, 0.001

Values written in the bold are taken from the existing STHE. To test the influence of decision variables over problem objectives back and forth of this values can be used.

Table 3.4 Diameter effects

D_i	**A**	**A_i**	**U**	**$\dot{Q}$**	**ΔP_{fs}**	**ΔP_{Tt}**
0.034	121.2632	27.00622	117.4943	797522.7	12475.31	327.1139
0.036	119.3312	27.3046	118.2336	794643.1	12583.11	292.1725
0.038	117.4376	27.54709	118.9084	791592.2	12684.63	262.4165
0.04	115.5827	27.73984	119.5268	788393.4	12780.23	236.9093
0.042	113.7665	27.88829	120.0955	785066.4	12870.24	214.9142
0.044	111.989	27.99726	120.6203	781627.7	12954.95	195.8455
0.046	110.2499	28.07101	121.1059	778091.5	13034.63	179.2329

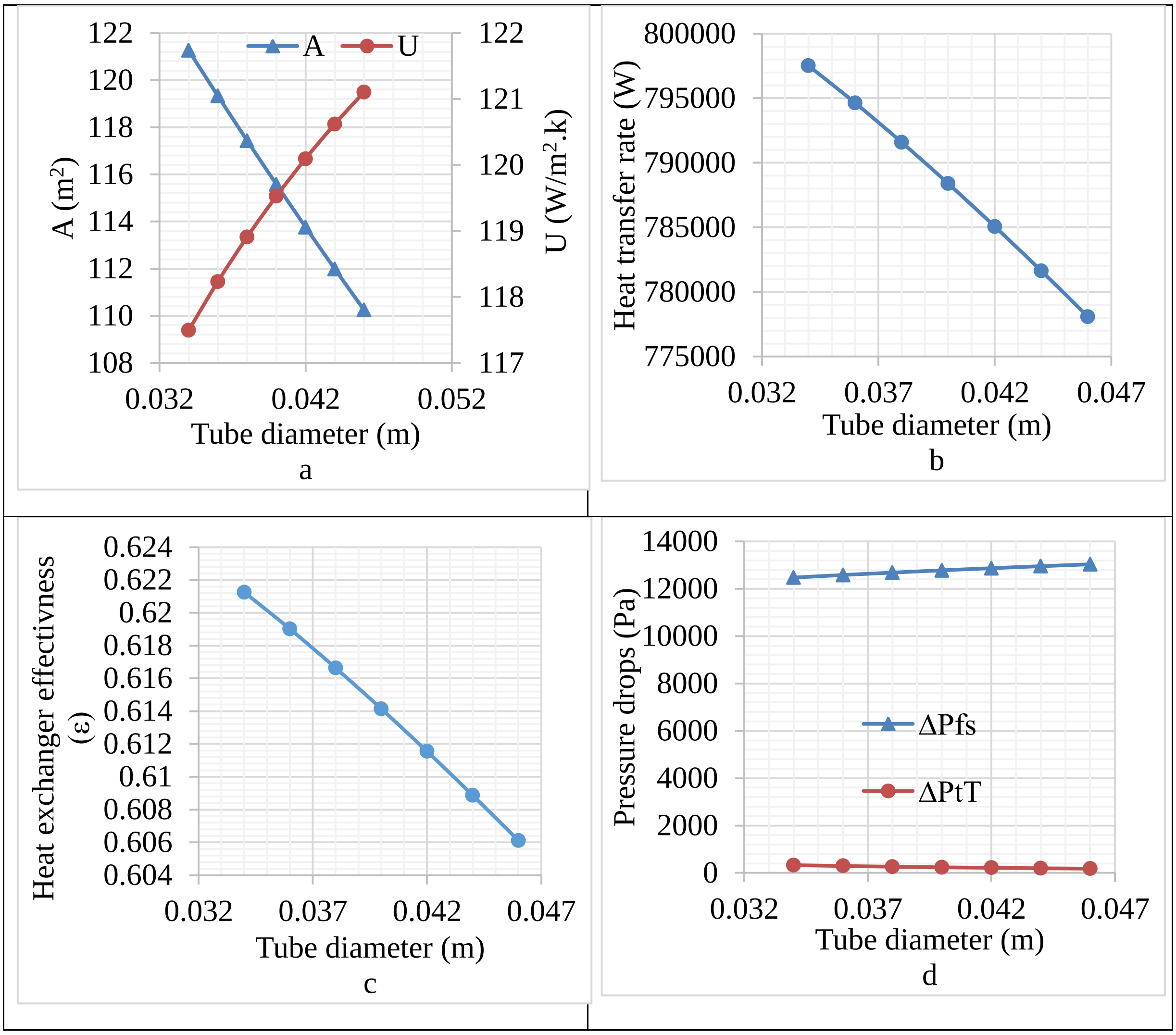

Figure 3.1 Effects of diameter on objective functions

As shown the fig. a-d above when internal diameter of the tube increases from 0.034 to 0.046 mm: overall heat transfer coefficient increase and blockage of gas in the shell is increase which leads pressure drop on the shell side are increasing in a small amount. Total area and heat exchanger effectiveness (heat transfer rate) decrease in a small amount. Here only pressure drop on the tube side is decreasing rapidly due to decrease of friction in the tube. The effects on heat transfer rate and heat exchanger effectiveness have the same profile since $\dot{Q} = 1.283731757 \times 10^6 \varepsilon$.

Table 3.5 Fin space effects

ℓ	A	η_w	U	$\dot{Q}$	ΔP_{fsT}
0.017	134.7694	0.799476	109.5587	807860	15241.76
0.019	127.3899	0.801304	113.0594	800682.3	14245.88
0.021	121.0646	0.803198	116.3745	794221.6	13442.56
0.023	115.5827	0.805139	119.5268	788393.4	12780.23
0.025	110.786	0.807109	122.5349	783124.5	12224.24
0.027	106.5536	0.809098	125.414	778351.6	11750.41
0.029	102.7915	0.811095	128.1768	774019.9	11341.41

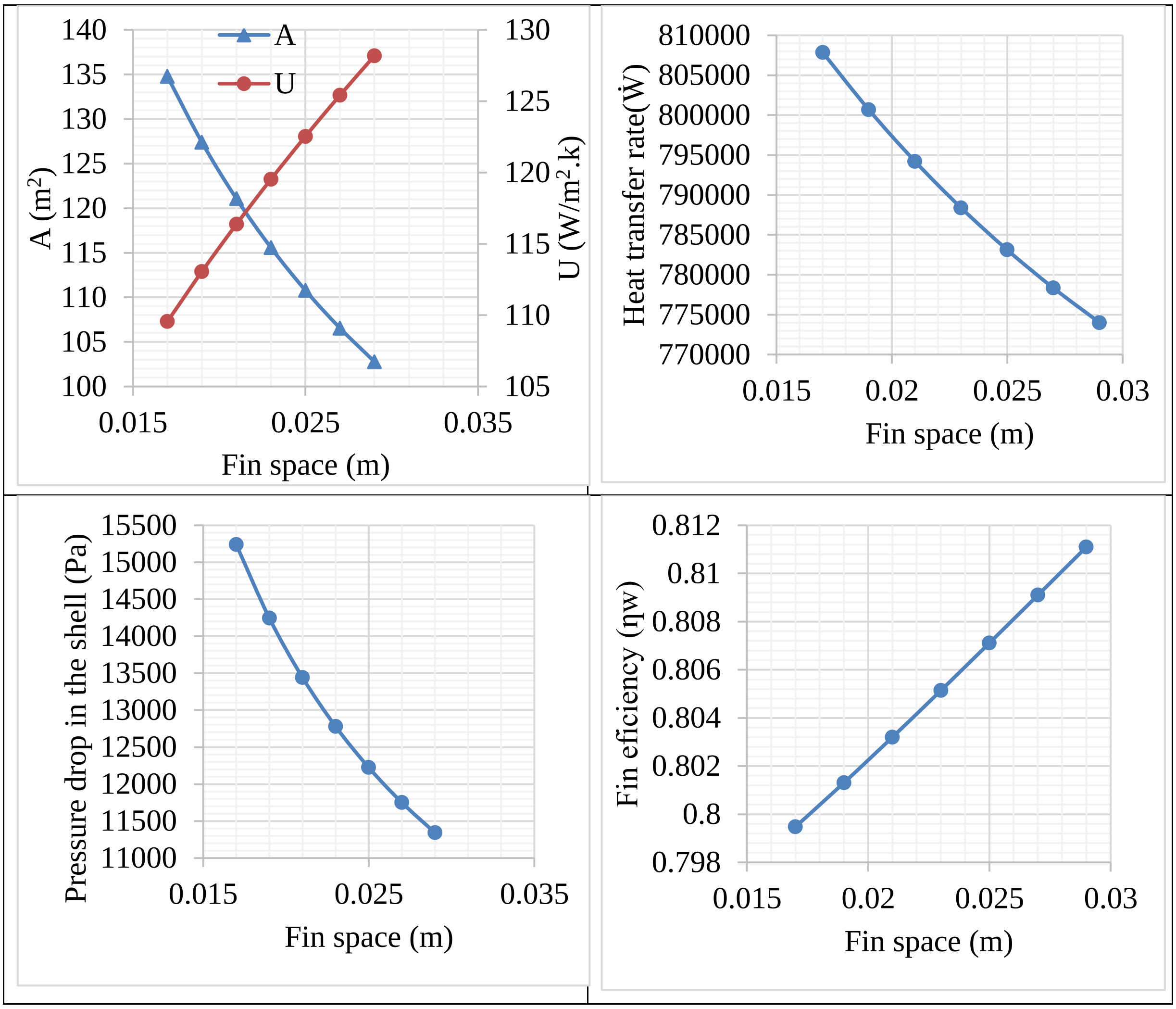

Figure 3.2 Effects of fin space on objective functions

Figure 3.2 shows that whenever the fin space increase from 0.017 to 0.029 mm:

- ✓ Area of heat exchanger decrease due to fin area decrease.
- ✓ Overall fin efficiency $\eta_w = \frac{A_b + \eta_f A_f}{A}$ improved with a very small amount because of heat transfer area decrease but individual fin efficiency decrease.
- ✓ Overall Heat transfer coefficient increase due to overall fin efficiency increase.
- ✓ Shell side pressure drop decrease due to less turbulence in the shell.
- ✓ But heat transfer rate decrease moderately compared to values on diameter.

Table 3.6 Fin height effects

b	A	Ai	η_w	U	$\dot{Q}$	ΔP_{fsT}	ΔP_{Tt}
0.014	117.3681	36.71576	0.878688	153.069	859786.1	18925.84	314.5016
0.016	116.7938	33.30621	0.854756	140.2836	836498.8	16377.88	285.0278
0.018	116.1963	30.33845	0.830114	129.2201	812632.7	14380.95	259.3729
0.02	115.5827	27.73984	0.805078	119.5268	788393.4	12780.23	236.9093
0.022	114.9584	25.45205	0.779921	110.9512	763965.3	11472.63	217.1325
0.024	114.3277	23.4278	0.754875	103.3058	739513.4	10387.18	199.6339
0.026	113.6935	21.62844	0.730134	96.44731	715184.1	9473.61	184.0793

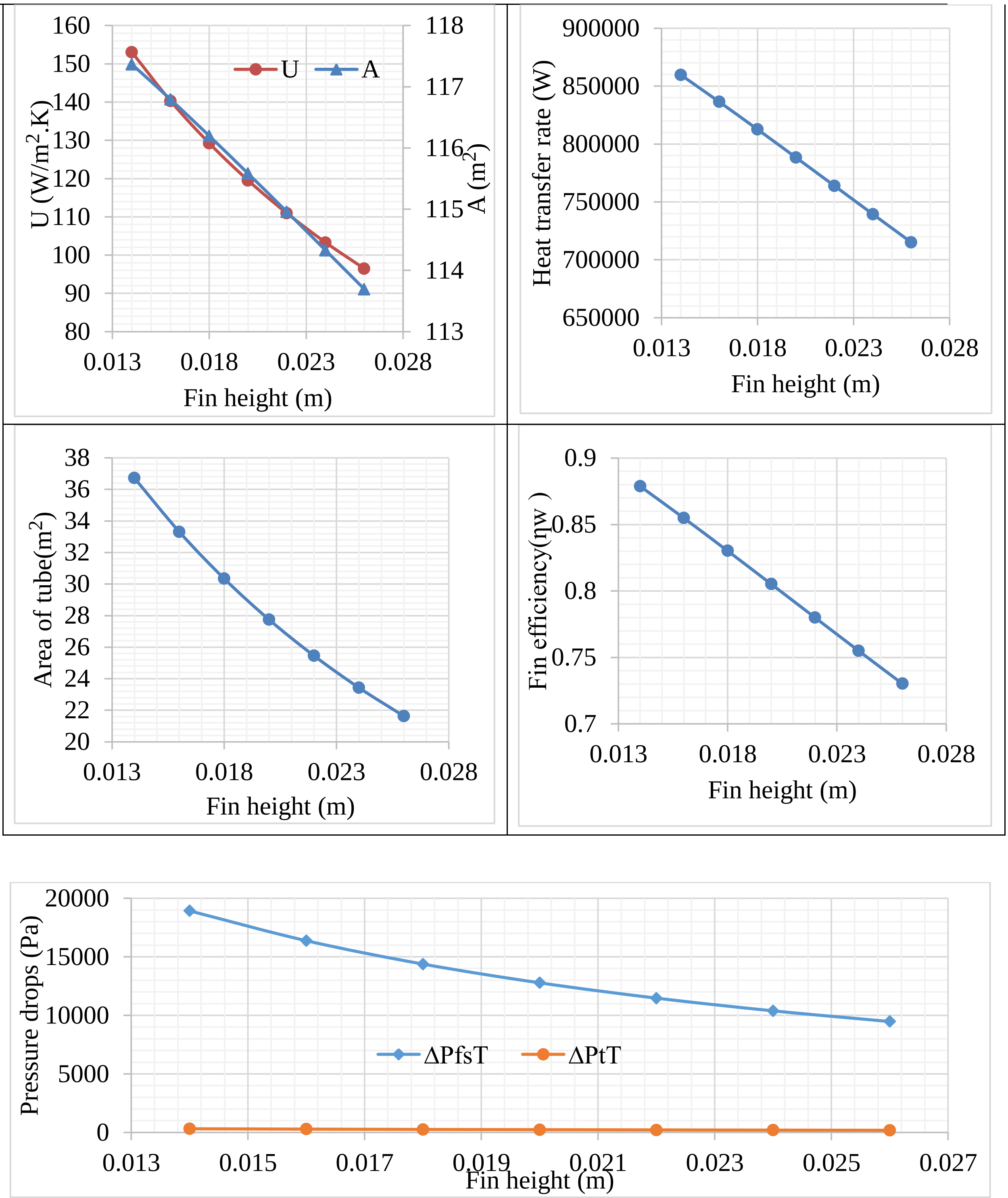

Figure 3.3 Effects of fin height on objective functions

Table 3.7 Effects of fin thickness

τ	A	η_w	U	$Q^{\cdot}$	ΔP_{fsT}
0.001	127.8344	0.563536	96.5455	753603.1	9508.287
0.003	123.1222	0.713878	109.7159	781634.5	10595.38
0.005	119.0832	0.774121	115.6901	787558.7	11687.29
0.007	115.5827	0.805139	119.5268	788393.4	12780.23

0.009	112.5197	0.823193	122.4266	787529.6	13871.03
0.011	109.8171	0.834408	124.803	786003.8	14957.04
0.013	107.4148	0.841587	126.836	784210	16036.07

As shown values above from table and graph fin height has more variational effects. When fin height increase from 0.014 to 0.026 mm fin efficiency, heat transfer coefficient, heat transfer rate and pressure drop both on shell and tube side are increasing rapidly whereas total area change is small almost negligible.

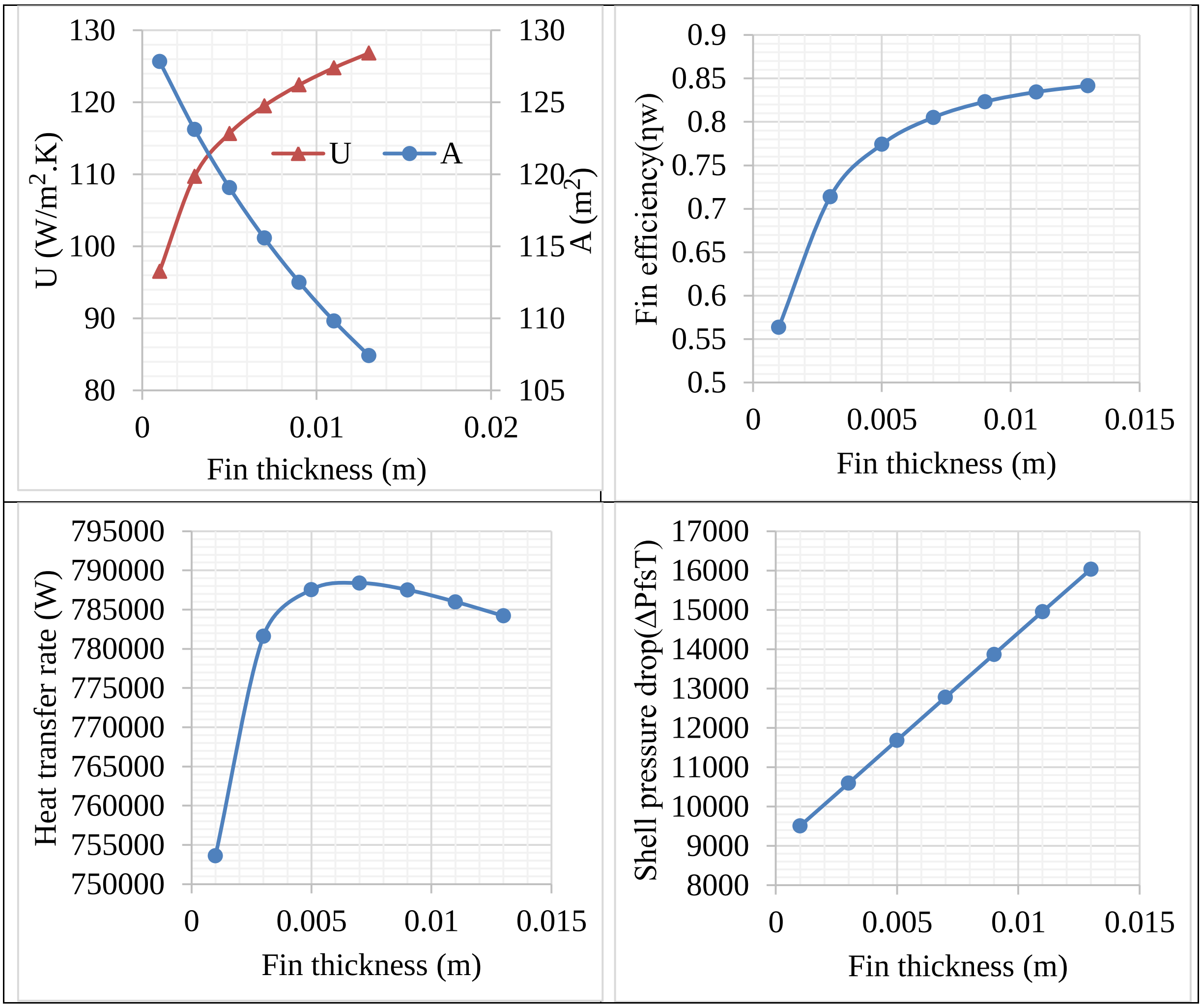

Figure 3.4 Effects of fin thickness on objective functions

Table 3.7 and fig.3.4 shows that whenever fin thickness increases from 0.011 to 0.013:

- ✓ Fin efficiency, heat transfer coefficient and shell side pressure drop also increases. But pressure drop increase more rapidly
- ✓ Total surface area of STHE decrease.
- ✓ Heat transfer rate first increases after a while it is decreasing but in a very small amount almost negligible.

In optimizing, the sensibility analysis needs to decide which adjustable variables of the problem are more important than others. Depending on sensitivities of variables over the objective functions, inside tube diameter and fin thickness have no significant effect on heat transfer rate. But fin height is more sensitive over the heat transfer rate and pressure drops which is related to operating cost. Fin space also more sensitive on heat transfer rate than fin thickness and diameter. Therefor from these result decision variables can be reduced to two decrease problem complexities that is:

- ✓ Fin height and
- ✓ Fin space.

By using these two decision variables design optimization of STHE can be performed.

4. RESULTS AND DISCUSSION

4.1. Comparison of Univariate Results

From sensitivity analysis, all values of heat transfer rate and heat exchanger performances are greater than constraint values set above, which is due to change of tube layout. Therefore, for the next analysis calculated by the two decision variables (fin height and fin space) can be unconstrained univariate optimization type.

Table 4. 1 Selected decision variables and their range

Decision variables	Range(m)
Fin height (b)	0.011, 0.014, 0.017, **0.02**, 0.023, 0.026, 0.029
Fin spacing (ℓ)	0.014, 0.017, 0.02, **0.023**, 0.026, 0.029, 0.032

In Table 4.1, there are two variables, fin height (b) and fin spacing (ℓ) which have seven different values. By using these different values, 49 different alternative shell and tube heat exchanger can be found.

These 49 different solutions are there. From which some required parameter values are single out and presented in Tables below.

Table 4.2. Effects of fin height (b) and fin space (ℓ) over heat transfer area

ℓ (m)	Heat transfer area (m^2)						
b (m)	**0.014**	**0.017**	**0.02**	**0.023**	**0.026**	**0.029**	**0.032**
0.011	143.0868	132.7023	124.6254	118.1639	112.8773	108.4717	104.744
0.014	145.6392	133.8596	124.6976	117.3681	111.3712	106.3737	102.1451
0.017	147.3617	134.5016	124.4993	116.4974	109.9505	104.4947	99.87822
0.02	148.4742	134.7694	124.1101	115.5827	108.6057	102.7915	97.87184
0.023	149.1309	134.7612	123.5848	114.6436	107.3282	101.2319	96.07359
0.026	149.4422	134.5469	122.9617	113.6935	106.1104	99.7912	94.44417
0.029	149.4886	134.177	122.268	112.7408	104.9458	98.45004	92.95358

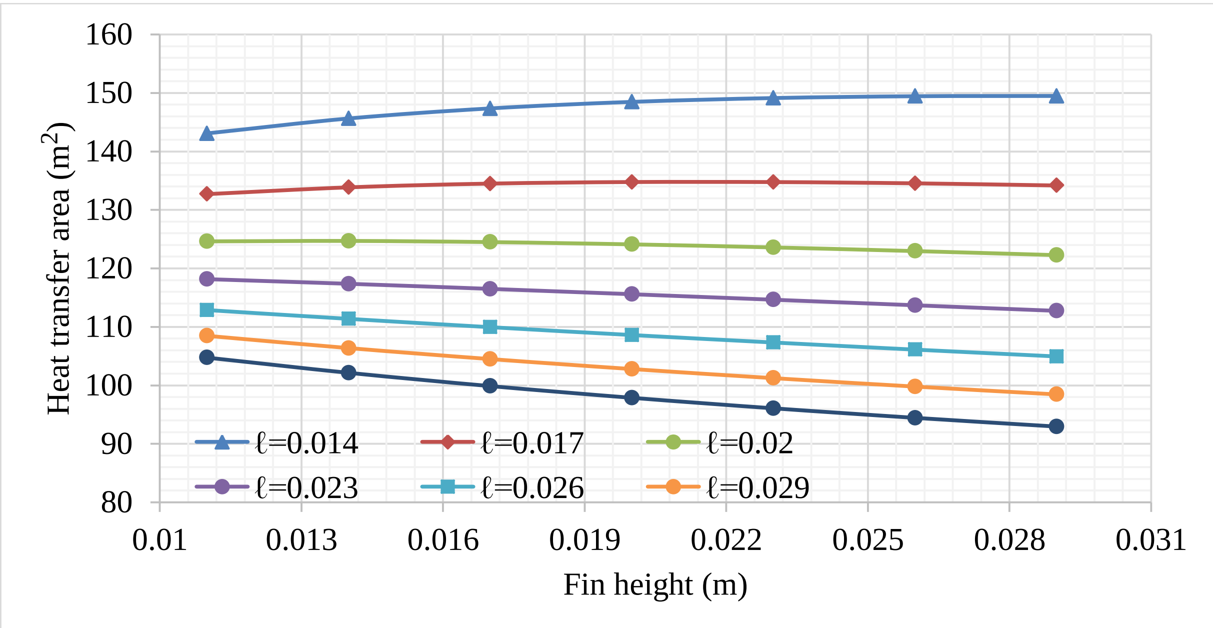

Figure 4.1 Effects of fin height and space over heat transfer area

As Figure 4.1 shows, for smaller constant fin space when fin height increase, fin area increase and base areas decrease with equivalent range as fin area due to number of tubes in the shell decrease. But the sum of the two that is total heat transfer area increase in a small amount.

For higher constant fin space when fin height increase, fin area increase in smaller range and base area decrease with a greater range than fin area. Therefore heat transfer area decrease for higher fin space.

Table 4. 2 Effects of fin height (b) and fin space (ℓ) over overall heat transfer coefficient

ℓ (m) / b (m)	Overall heat transfer coefficient (W/ m².K)						
	0.014	**0.017**	**0.02**	**0.023**	**0.026**	**0.029**	**0.032**
0.011	156.024	163.6118	170.4395	176.659	182.3778	187.6754	192.6129
0.014	134.3433	141.1872	147.3873	153.069	158.3215	163.2113	167.7895
0.017	117.4813	123.6941	129.3519	134.5615	139.3991	143.9214	148.1722
0.02	103.8941	109.5587	114.7386	119.5268	123.9897	128.1768	132.1261
0.023	92.67636	97.85839	102.6128	107.022	111.1447	115.0248	118.6956
0.026	83.2522	88.00631	92.38008	96.44731	100.2607	103.8594	107.2733
0.029	75.23134	79.60439	83.63675	87.39519	90.92741	94.26871	97.44594

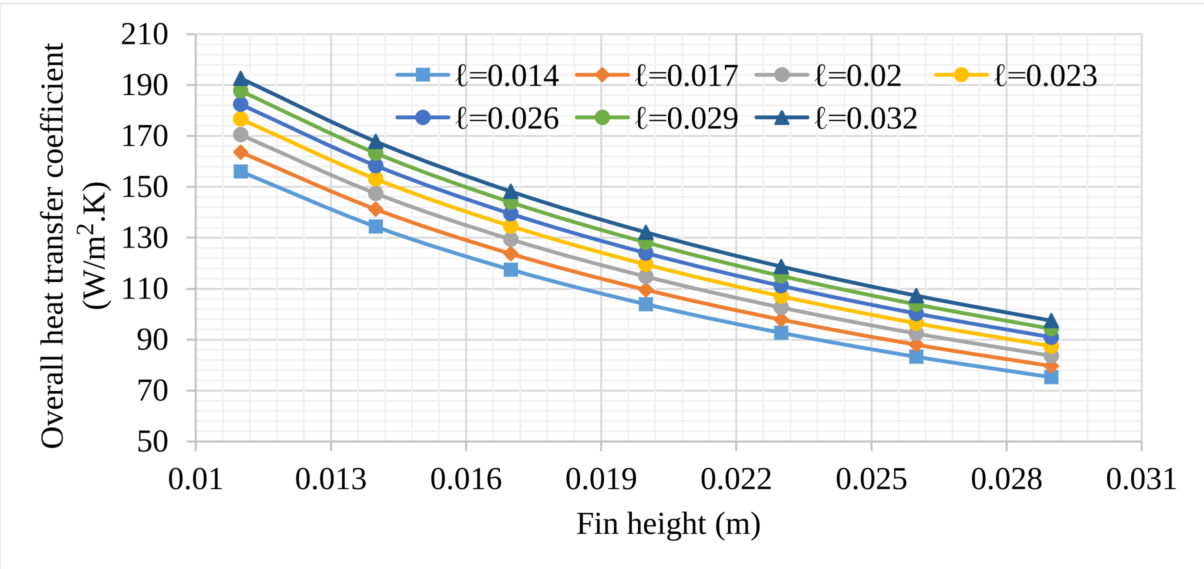

Figure 4. 2 Effects of fin height and space over heat transfer coefficient

Figure 4.2 tells that: At constant fin space, overall heat transfer coefficient decrease with increasing of fin height and at constant fin height heat transfer coefficient increase as fin space increase. But it increases with a small amount.

Table 4. 3 Effects of fin height (b) and fin space (ℓ) over fin efficiency

ℓ (m) / b (m)	Overall fin efficiency (η_w)						
	0.014	**0.017**	**0.02**	**0.023**	**0.026**	**0.029**	**0.032**
0.011	0.905199	0.907663	0.910115	0.912507	0.914818	0.917037	0.919159
0.014	0.870785	0.873391	0.87606	0.878731	0.881365	0.883941	0.886447
0.017	0.834337	0.836963	0.839727	0.842555	0.845401	0.84823	0.851023
0.02	0.796912	0.799476	0.802244	0.805139	0.808102	0.811095	0.814088
0.023	0.759381	0.761831	0.764545	0.767438	0.77045	0.773534	0.776654
0.026	0.722428	0.724739	0.72736	0.730207	0.733216	0.736335	0.739525
0.029	0.686563	0.688725	0.691234	0.694006	0.696976	0.700089	0.703303

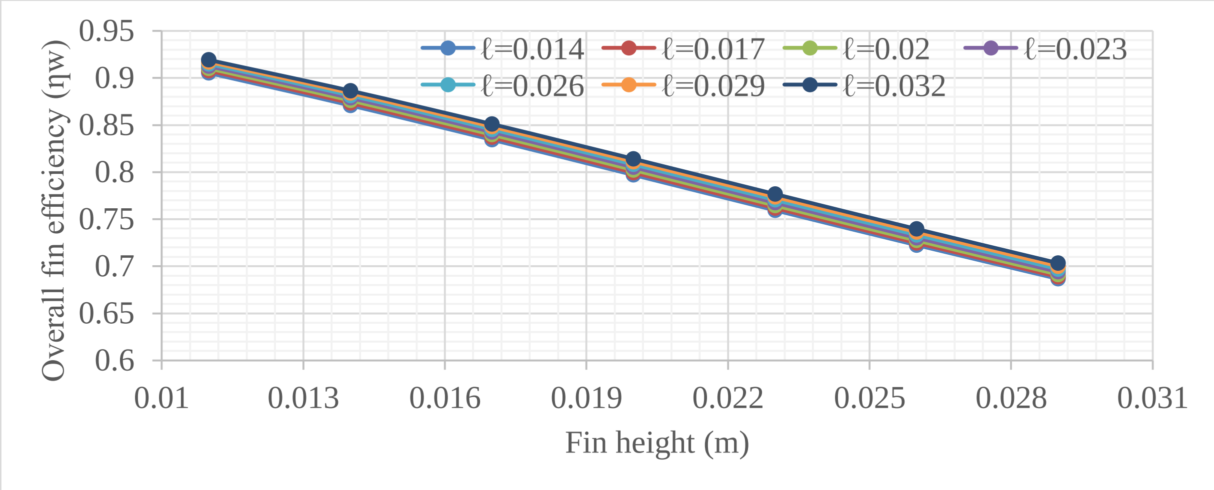

Figure 4. 3 Effects of fin height and fin space over fin efficiency

From figure 5.3: At constant fin space with increasing of fin height, fin efficiency is decreasing more rapidly.

Table 4. 4 Effects of fin height (b) and fin space (ℓ) over heat transfer rate

ℓ (m) / b (m)	Heat transfer rate (W) 0.014	0.017	0.02	0.023	0.026	0.029	0.032
0.011	906074.9	900850	896590.9	893115.7	890277.7	887959.7	886068.3
0.014	879461.9	871698.4	865215.6	859786.1	855224.5	851381.4	848136.5
0.017	850671.5	840509.6	831918.3	824624.7	818407.1	813086.5	808518.3
0.02	820188.6	807860	797367.9	788393.4	780679.6	774019.9	768247.5
0.023	788516.3	774300.1	762160.2	751732.7	742727.1	734911	728097.3
0.026	756147.4	740340.2	726821.5	715184.1	705105.9	696331.1	688654.6
0.029	723538	706435.1	691803.6	679195.5	668260.7	658722.5	650359.9

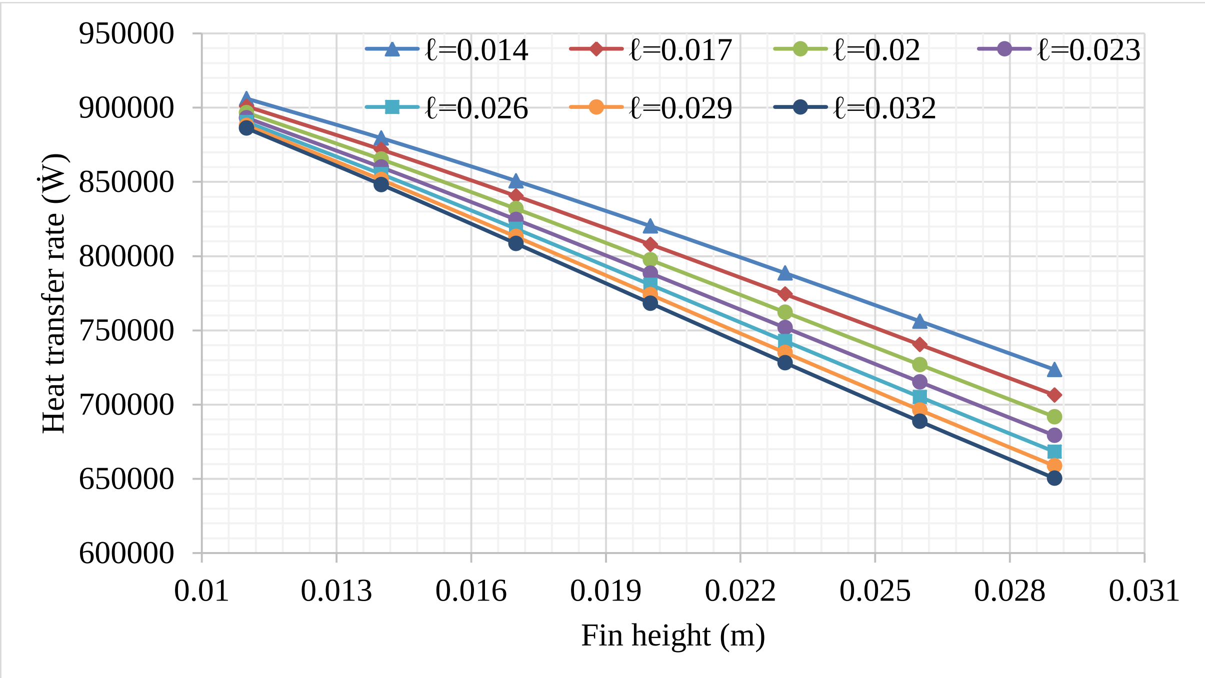

Figure 4. 4 Effects of fin height and fin space over heat transfer rate

Heat transfer rate:

At constant fin height with increasing of fin space, rate of heat transfer is decreasing in a very small amount especially for smaller fin height.

Table 4. 5 Effects of fin height (b) and space (ℓ) over pressure drop on the shell side

ℓ (m) / b (m)	Pressure drop on the shell side (Pa) 0.014	0.017	0.02	0.023	0.026	0.029	0.032
0.011	31596.07	28352.97	26060.29	24349.31	23020.26	21955.61	21081.71
0.014	24990.63	22260.77	20346.14	18925.84	17827.79	16951.58	16234.69
0.017	20503.29	18161.02	16527.9	15321.74	14392.45	13652.94	13049.29
0.02	17284.76	15241.76	13823.87	12780.23	11978.26	11341.41	10822.44
0.023	14878.36	13071.72	11822.57	10905.66	10202.55	9645.12	9191.471
0.026	13019.34	11403.24	10289.36	9473.61	8849.147	8354.737	7952.808
0.029	11544.81	10085.14	9081.777	8348.401	7787.816	7344.483	6984.398

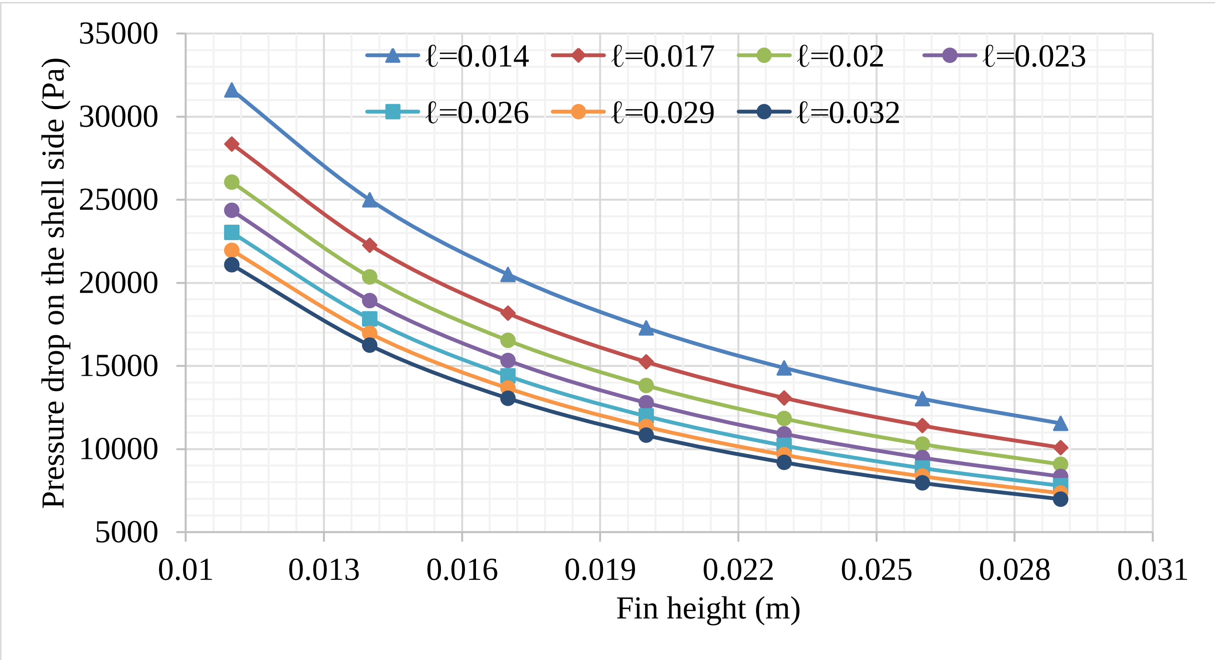

Figure 4. 5 Effects of fin height and fin space over pressure drop on the shell side

Pressure drops:

Whenever the fin space increase at constant fin height, pressure drop decrease. But the rate of decreasing of pressure drop decrease.

At constant fin space decreasing of pressure drop rates are decrease with increasing fin height.

Now conclusion can be drown that at 32 mm fin space, pressure drops and heat transfer area are decreased with a small heat transfer rate penalty. But at constant 32 mm there are 7 alternative solution as yet. Which is

Table 4. 6 Values at 32 mm fin space and variable fin heights.

b	A	η_w	U	Q˙	ΔP_{fsT}	ΔP_{Tt}
0.011	104.744	0.919159	192.6129	886068.3	21081.71	367.6569
0.014	102.1451	0.886447	167.7895	848136.5	16234.69	314.5016
0.017	99.87822	0.851023	148.1722	808518.3	13049.29	271.7655
0.02	97.99125	0.814088	131.9791	768280.4	10592.62	215.4998
0.023	96.07359	0.776654	118.6956	728097.3	9191.471	208.1208
0.026	94.44417	0.739525	107.2733	688654.6	7952.808	184.0793
0.029	92.95358	0.703303	97.44594	650359.9	6984.398	163.8035

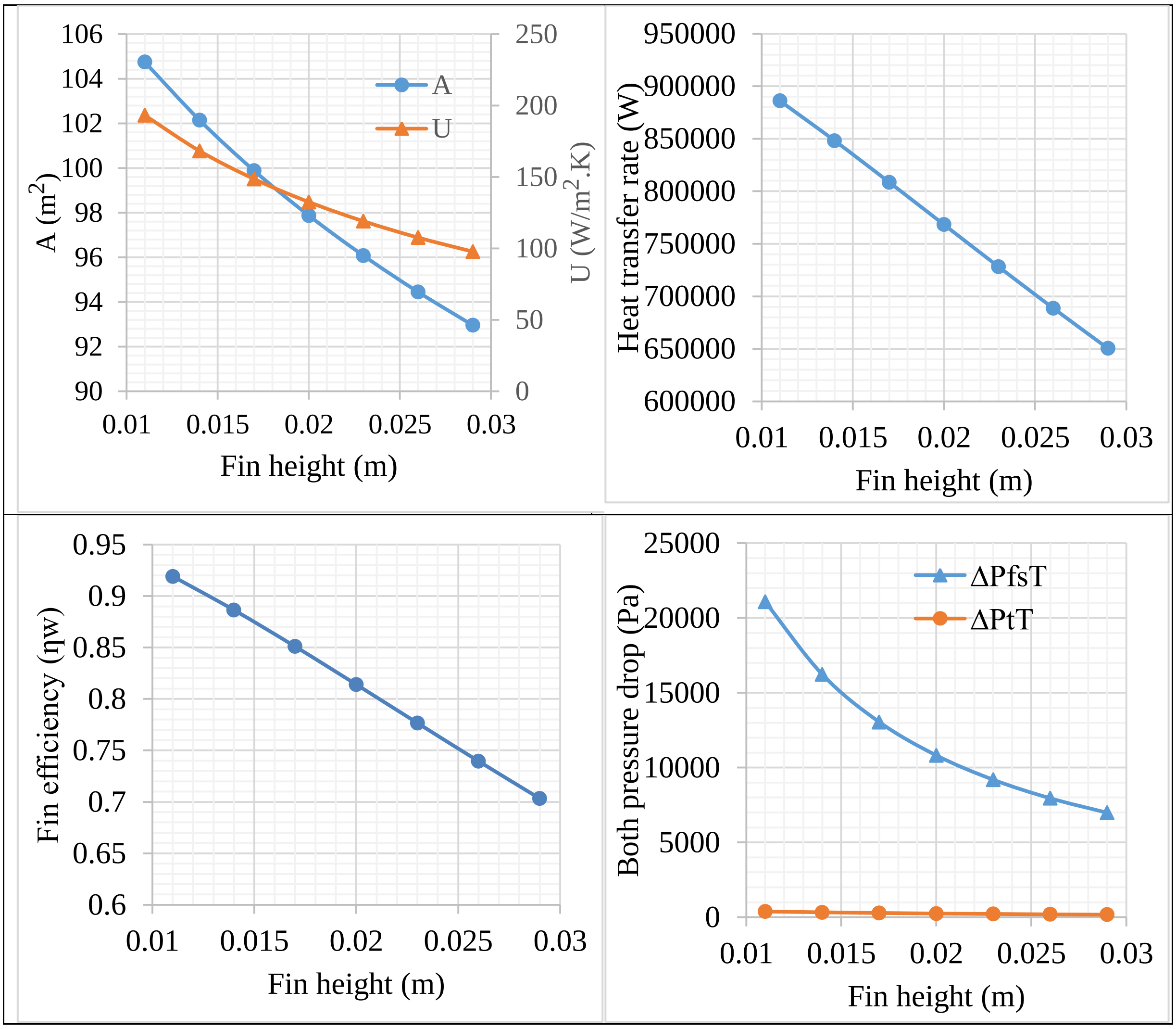

Figure 4. 6 Area, heat transfer coefficient, heat transfer rate, efficiency and pressure drops at a constant 32 mm fin space.

To select the best values to fulfill the objective functions, total cost evaluation has to be required. Functional years of original (existing) STHE (n_y) = 20 years, annual discount rate (i) = 10 %, unit price of electrical energy (Kel) = 0.06 $\$/kWh$ [Energy4sustainablefuture.blogspot.com], Pump efficiency $\eta = 75\ \%$ *and* the hours of operation per year(H) = 8040 h/year (The remaining days being nominal maintenance shutdown days).

Then by using cost estimation equations, 7 different alternative calculated values are listed in the table below.

Table 4. 7 Investment cost, operating cost and total cost

b (m)	C_{in} (\$)	C_{op} (\$)	C_T (\$)
0.011	72406.4275	3050221.19	3122627.61
0.014	71657.9338	2348930.64	2420588.58
0.017	71002.7095	1888049.46	1959052.17
0.02	61425.2315	1532500.12	1593900.35
0.023	69898.0155	1329880.1	1399778.12
0.026	69422.9297	1150663.3	1220086.23
0.029	68987.2596	1010548.22	1079535.48

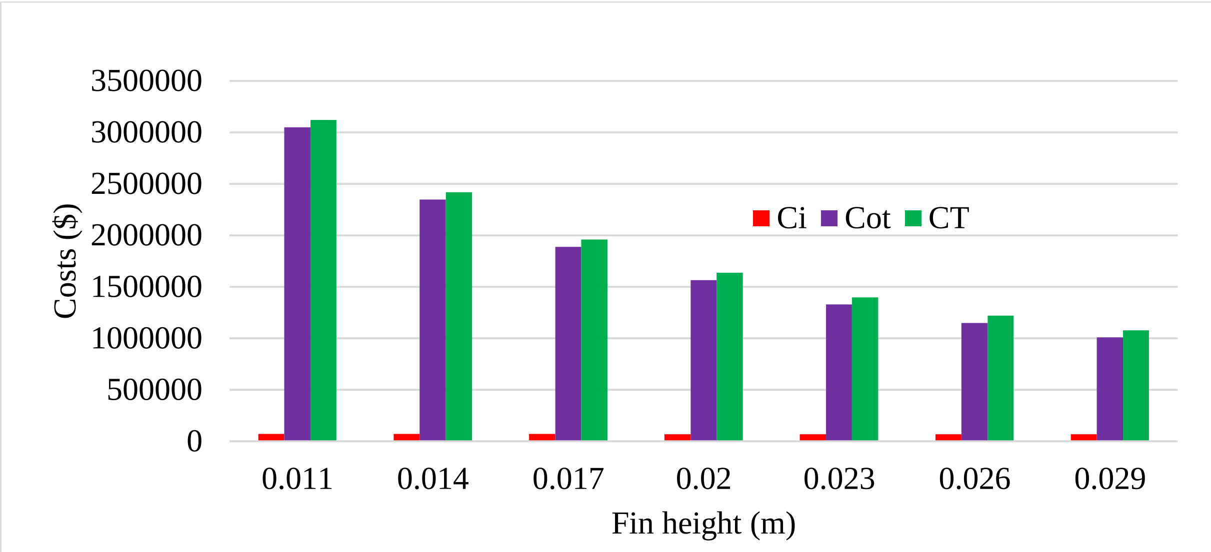

Figure 4. 7 Capital, operational and total cost of STHEX

Table 4.8 suggests that whenever fin height values varies from 11mm to 29 mm at constant 32 mm fin space there is no significant change on investment cost this means there is no significant change on heat transfer area. But not on operational cost. Figure 5.7 indicates that operating cost is the dominant cost factor in a shell and tube heat exchanger. Even if it incorporates pumping cost for hot and cold fluids, the dominant factor for this cost is pumping cost of hot fluid in the shell. As a result to minimize total cost it is better to focus on pressure drop in the shell which is responsible for operational cost.

4.2 Dual Objective Optimization Using Univariate Method

As mentioned, dual objective optimization yields Pareto solutions that constructs the Pareto curve. It can also be said that a favorable trade-off between the results of contradictive objectives is called Pareto optimum solution. Figure 5.8 and 5.9 shows the Pareto frontier constructed by the dual objective optimization of abovementioned problem objectives.

Table 4. 8 Pareto optimal solution

CT (\$)	$\dot{Q}$ (W)
3122627.61	886068.3
2420588.58	848136.5
1959052.17	808518.3
1593900.35	768280.4
1399778.12	728097.3
1220086.23	688654.6
1079535.48	650359.9

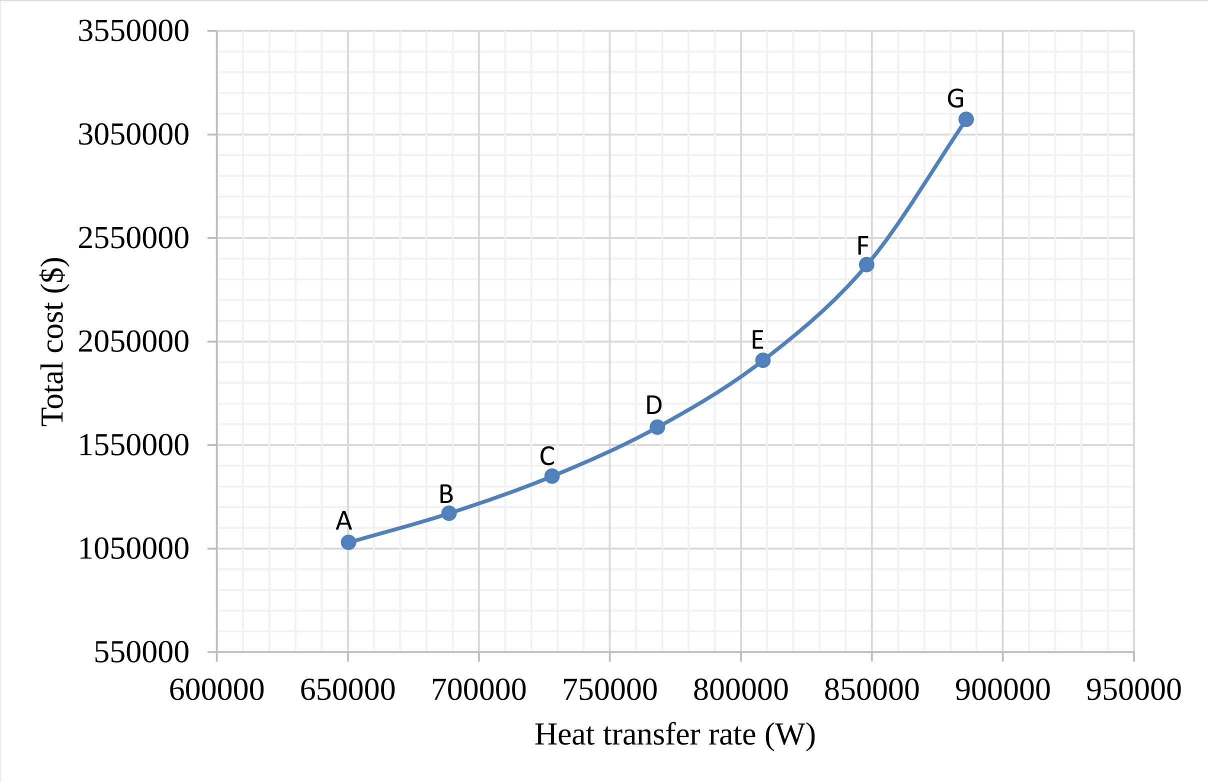

Figure 4. 8 Pareto curve of objective function

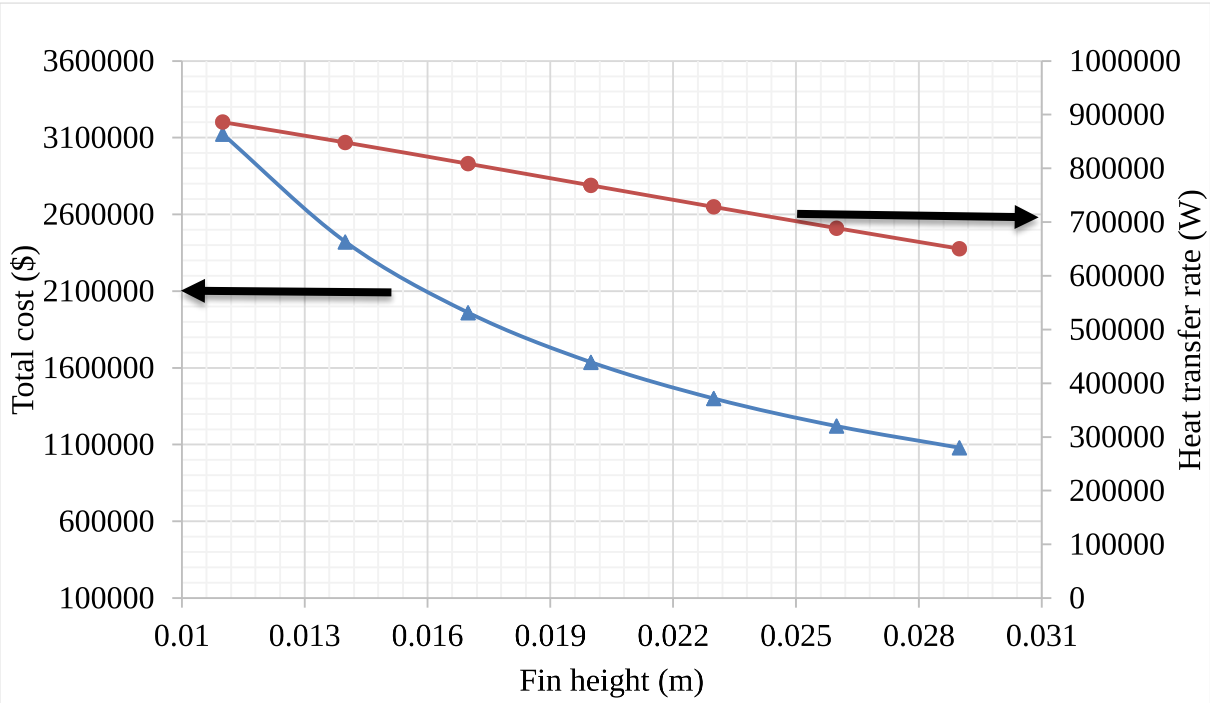

Figure 4. 9 Heat transfer rat and total cost at different fin height

Univariate optimization technique was implemented using Excel to get optimal solutions and for these optimal solutions Pareto analysis is required to decide important adjustable variables. As shown Figure 5.8 on the Pareto curve which indicates the conflict between total cost and heat transfer coefficient that is at point A both cost and heat transfer rate are minimum whereas at point G both objective functions are maximum.

Figure 4.9 indicate that whenever increasing fin height from 11 mm to 29 mm heat transfer rate decrease almost in equal ranges, while total cost drops rapidly for the first some values. But the range of decreasing values become decrease with fin height.

Finally, from Pareto optimal point solutions one point can be selected for constraint of $\dot{Q} \geq 5.133\times10^5$ W and CT ≤ 1.8294×10^6 \$. Due to this, it is acceptable to choose design point D at $\dot{Q} = 7.6828\times10^5$ W and CT=1.5939×10^6 \$ as modified design of shell and tube heat exchanger of for univariate optimization method.

4.3 Dual Objective Optimization Using ACO

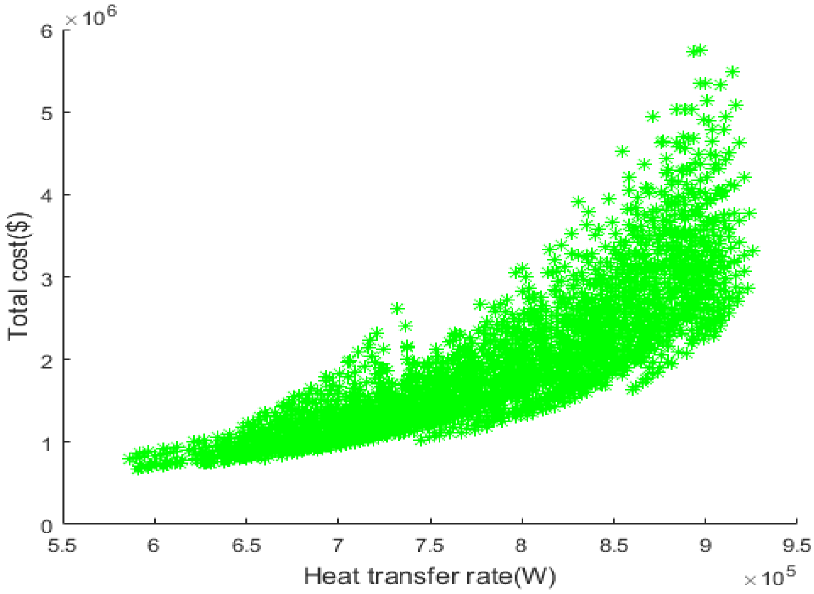

Figure 5. 10 Total cost Vs heat transfer rate Pareto fronts of STHEs without constraints.

When constraint parameters are excluded (non-constraint optimization) as shown Figure 5.10, 2,401 alternative number of STHEs which represented with its' total cost and heat transfer rate can be found by using MATLAB code.

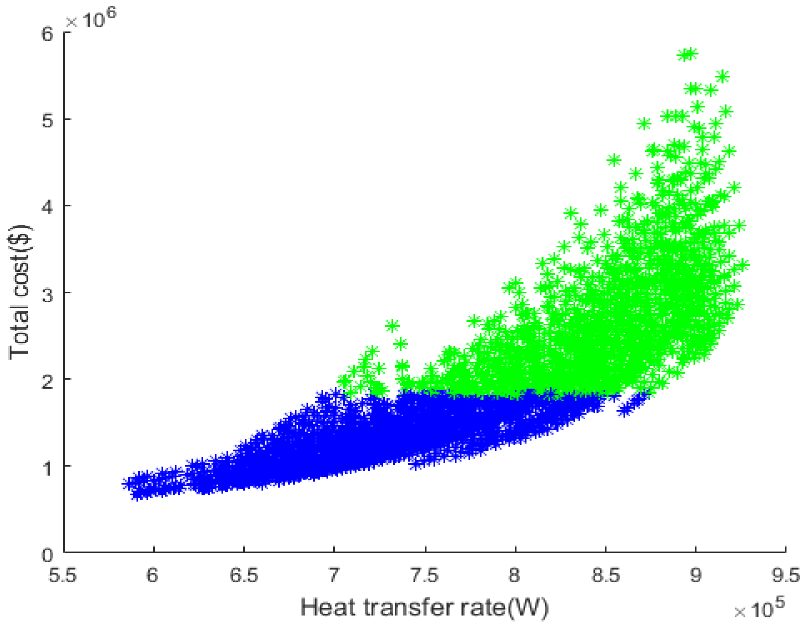

Figure 4. 11 Total cost Vs heat transfer rate Pareto fronts of STHEs for CT ≤ 1.8294×10^6 and CT ≥ 1.8294×10^6 \$ which is existing STHE cost estimation.

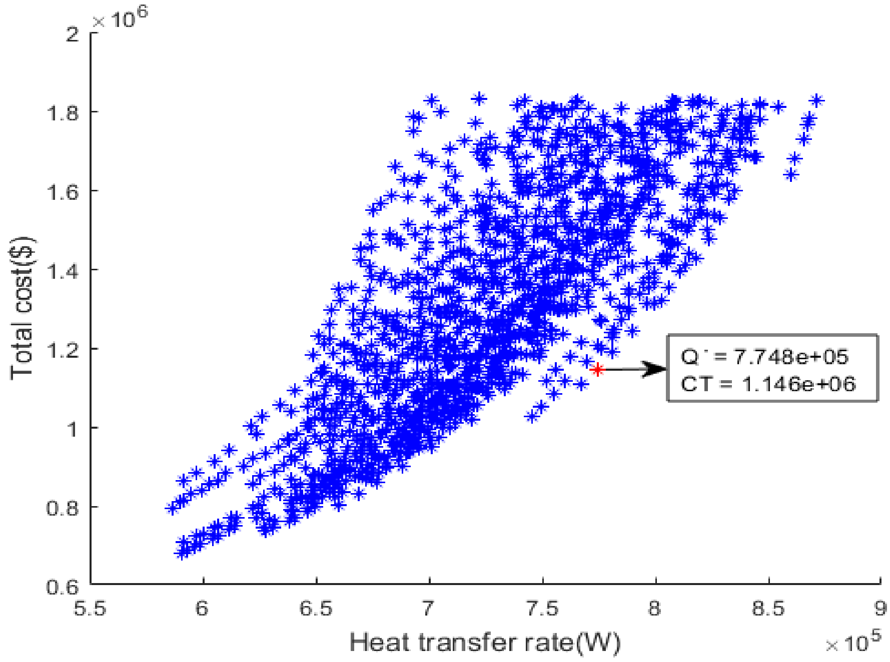

Figure 4. 12 Total cost Vs heat transfer rate Pareto front of STHEs with constraint of $\dot{Q} \geq 5.133\times10^5$ W and CT ≤ 1.8294×10^6 \$.

As Figure 4.10, the stares in Figure 4.12 also shows different alternative STHEs. But it has constraint parameters of $\dot{Q} \geq 5.133\times10^5$ W and CT ≤ 1.8294×10^6 \$ which is taken from existing STHE. Due to this number of alternative, STHEs are decreased from 2,401 to 1,280. Of which one optimum point with the smallest total cost to heat transfer rate ratio (CT/$\dot{Q}$ = 1.4795) is selected. At this point total cost and heat transfer rate are 1.1463×10^6 \$ and 7.74810×10^5 W respectively.

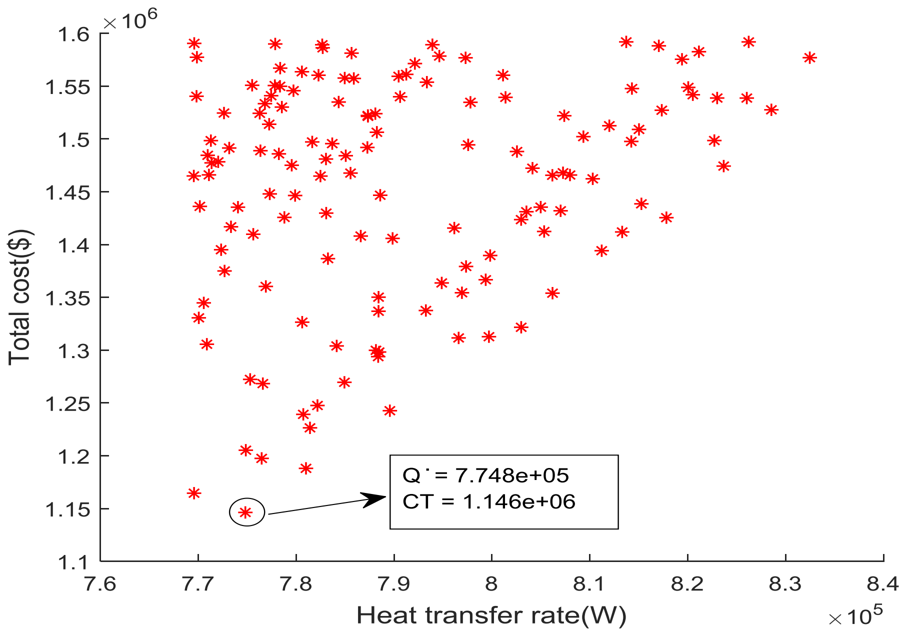

Figure 4. 13 Total cost Vs heat transfer rate Pareto front of STHEs with constraint of $\dot{Q} \geq 7.6828\times10^5$ W and CT ≤ 1.5939×10^6 \$.

If $\dot{Q} \geq 7.6828\times10^5$ W and CT ≤ 1.5939×10^6 \$ which is values of modified STHE calculated by univariate method is taken as constraints, 139 alternative heat exchangers can be found as shown in Figure 4.13.

Design optimization of heat exchanger by using Univariate and ACO have different optimal values. Existing parameter values and modified STHE optimal point values both in Univariate and ACO are listed below in Table 4.9.

Table 4. 9 Both existing and modified exchanger parameter values

Heat exchanger parameters	Existing STHEX values	Modified STHE values (Univariate method)	Modified STHEX values (ACO method)
Fin diameter D_f(m)	0.115	0.096	0.09
Root diameter D_r(m)	0.075	0.056	0.05
Tube diameter D_i(m)	0.04	0.04	0.034
Fin space ℓ(m)	0.023	0.032	0.029
Fin height b(m)	0.02	0.02	0.02
Fin thickness τ(m)	0.007	0.007	0.003
Number of fin per tube N_f(m)	74	55	31
Number of tube N_T(m)	64	102	114
Number of pass n_p(m)	2	3	3
Number of tube per pass	32	34	38
Number of row N_r(m)	16	23	21
Heat transfer area A(m^2)	94.54	97.991247	110.7173
Heat tran. coef. in tube h_i($W/m^2.k$)	696.6	4216.76577	5168.7
Heat tran. coef. in shell h_o($W/m^2.k$)	227	240.7993642	246.8468
Overall heat trans.coef U($W/m^2.k$)	63.5	131.9791486	119.3063
Heat exchanger performance ε	0.3811	0.598474276	0.6036
Heat transfer rate $\dot{Q}$(W)	5.27×10^5	7.6828×10^5	7.7481×10^5
Pressure drop in shell ΔP_{fsT}(kPa)	12.209	10.5926232	7.5361
Pressure drop in tube ΔP_{tT}(Pa)	156.861	215.4997537	448.3515
Number of tubes per rows (for odd and even respectively)	4, 4	5, 4	6, 5
Investment cost C_{in}($)	6.3102×10^4	6.1425×10^4	5.6051×10^4
Operating cost C_{op}($)	1.7663×10^6	1.5325×10^6	1.0903×10^6
Total cost CT($)	1.8294×10^6	1.5939×10^6	1.1463×10^6

The existing design and the modified STHE obtained using Univariate optimization approach and ACO method results are summarized in Table 4.9. The table demonstrates that the Univariate design approach and the ACO design approach can reduce the total cost compared to the original design approach. Quantitatively, a remarkable reduction in the total cost was achieved using the Univariate approach (by 12.87 %) and the Ant Colony Optimization approach (by 37.34 %) as compared to the original design, whereas heat transfer rate increased by 45.78 % and 47.02 % by using Univariate and ACO method respectively as compared to the original design. Therefore, design optimization of modified STHE by using ACO approach can be the best choice. The results found from univariate and ACO were selected from 49 and 2,401 alternative STHEs respectively. To get the same result in univariate technique as ACO values, Univariate technique needs 2,401 trials on Excel spreadsheet. But it is tedious and takes time and also leads to input data as well as output analysis error. That is why sensitivity analysis is used to avoid this challenge.

Result Validation

The present results in both of the optimization methods are able to provide equivalent STHE design to the related reference [9].

This related reference calculated for a fined STHE using a multi-objective optimization genetic algorism for the decision variables (tube arrangement, tube diameter, tube pitch ratio, tube length, numbers of tube, fin height, fin thickness and baffle spacing ratio) involved in optimization of the objective functions (maximum heat transfer rate and minimum total cost). In this case, the equipment life was taken n_y = 10 years; and the working hours H = 7500 h/year.

Whereas the present work calculated for a fined STHE using a multi-objective optimization ACO and Univariate methods for the decision variables (tube arrangement, tube diameter, fin height, fin thickness and fin space) involved in optimization of the objective functions (maximum heat transfer rate and minimum total cost). The equipment life was taken n_y = 20 years; and the working hours H = 8040 h/year.

As shown figure 4.14, distribution of Pareto-optimal point solutions in 4.14a forms a curve line because in genetic algorisms each iteration results are updated in the next iterations.

In ACO, Pareto-optimal point solutions are randomly distributed, because of all iteration outputs are displayed. But as shown figure 4.14 all graphs have similar trend. Finally, by considering those conditions which make difference, these multi objective optimization methods for STHE design can be validated against the reference cases in the literature [9].

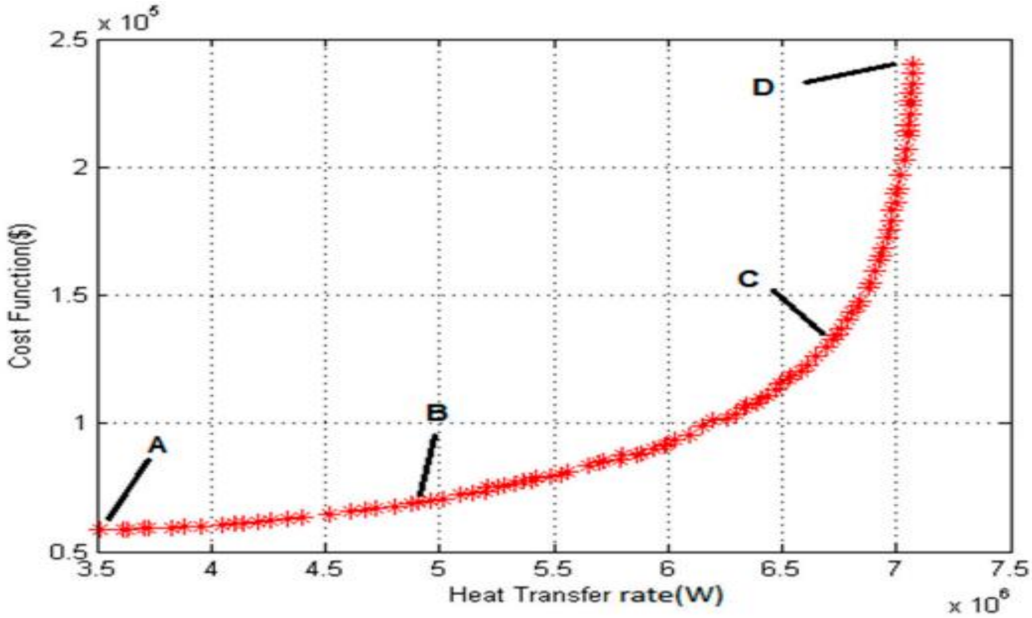

a). The distribution of Pareto-optimal point solutions using NSGA-II [9]

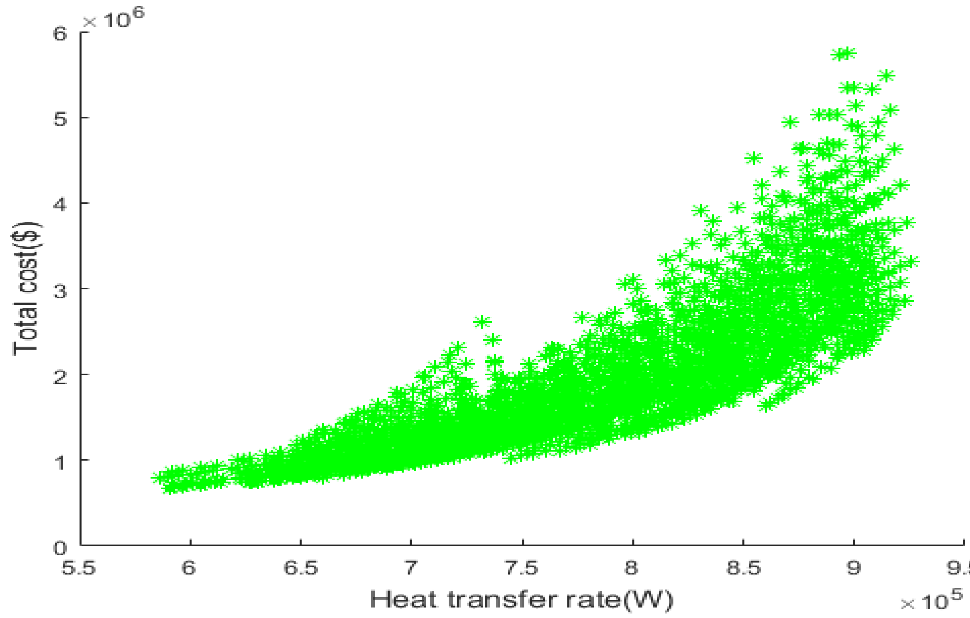

b). The distribution of Pareto-optimal point solutions using ACO

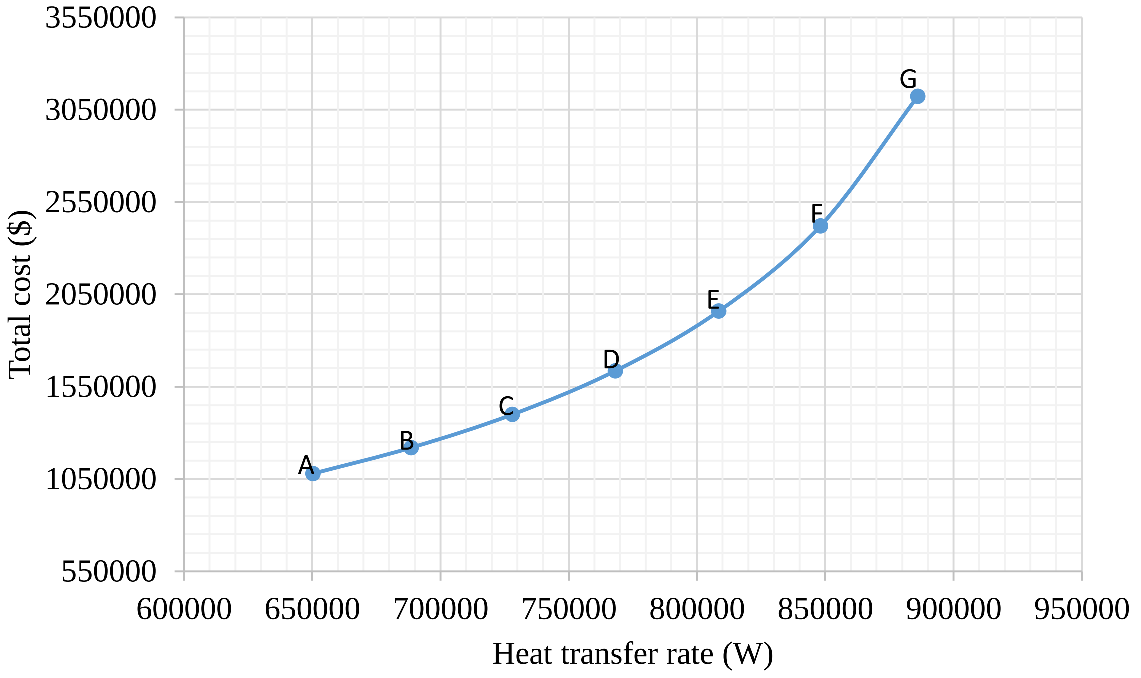

c). The distribution of Pareto-optimal point solutions using Univariate method

Figure 4. 14 Validation of present results against the reference cases in the literature

5. CONCLUSIONS

In this paper detail study of existing shell and tube heat exchanger and a modified multi-objective optimization design approach is proposed for the shell and tube heat exchanger on Microsoft Excel using univariate and ACO optimization technique with the objective functions of maximizing heat transfer rate and minimizing total cost using MATLAB. Five independent decision variables are considered, including tube arrangement, tube diameter, fin height, fin thickness and fin space. Of which, tube diameter and fin thickness have less significant change over heat transfer rate and multi objective optimization for the modification of a shell-and-tube heat exchanger allowed finding Pareto fronts with optimal decision variables both in Univariate(in Excel) and ACO(in MATLAB) techniques. From which it can be chosen one solution from all Pareto optimal solutions based on heat transfer rate as well as the cost of the design for both techniques. In Univariate and ACO methods, heat transfer rate (7.6828×10^5 W and 7.7481×10^5 W) and total cost (1.5939×10^6 $ and 1.1463×10^6 $) respectively have been selected.

Finally result shows that:

- The tube arrangement and fin height have more significant effects on heat transfer rate and cost of STHE.
- Operating cost is the dominant cost factor in a shell and tube heat exchanger.
- Within operating cost, pressure drop in the shell is a dominant factor.
- Heat transfer rate in both techniques have almost the same values, but it has significant difference in total cost.
- ACO approach is more cost-effective than Univariate (traditional) optimization technique.

Optimal point selected from Pareto optimal solutions of modified STHE in ACO approach was improves heat transfer rate by 47.02 % and total cost reduction by 37.34 % when compared with existing shell and tube heat exchanger.

6. REFERENCES

[1]. Shravan H. Gawande, Sunil D. Wankhede, Rahul N. Yerrawar, Vaishali J. Sonawane and Umesh B. Ubarhande, Design and Development of Shell and Tube Heat Exchanger for Beverage, Modern Mechanical Engineering, 2012, 2, 121-125.
[2]. Shah, R. K, Classification of Heat Exchangers, 1981.

[3]. Ramesh K. Shah, Fundamental of Heat Exchanger Design, Rochester Institute of Technology, Rochester, New York, 2003.
[4]. Usman Ur Rehman, Heat Transfer Optimization of Shell-and-Tube Heat Exchanger through CFD Studies, Chalmers University of Technology, G Oteborg, Sweden 2011.
[5]. Piyush Gupta, Avdhesh Kr. Sharma and Raj Kumar, Thermal Design of Shell and Tube Heat Exchanger Using Elliptical Tube, International Journal of Engineering and Manufacturing Science. ISSN 2249-3115 Vol. 7, 2017.
[6]. R. K. Shah, Heat Exchangers, in Encyclopedia of Energy Technology and the Environment, edited by A. Bisio and S. G. Boots, pp. 1651-1670, John Wiley & Sons, New York, 1994.
[7]. Frank P. Incropera, Theodore L. Bergman, Adrienne S. Lavine and David P. Dewitt Fundamentals of Heat and Mass Transfer, Seventh Edition, 2011.
[8]. Robert W. Serth, Process Heat Transfer Principles and Applications, Texas A&M University-Kingsville, Kingsville, Texas, USA, First edition 2007.
[9]. Heidar Sadeghzadeh, Mehdi Aliehyaei and Marc A. Rosen, Optimization of a Finned Shell and Tube Heat Exchanger Using a Multi-Objective Optimization Genetic Algorithm, ISSN 2071-1050, 25 August 2015.

NOMENCLATURES

List of Symbols and Abbreviations

Symbols

$\dot{Q}$	heat transfer rate [W]	N_f	number of fins [-]
$\dot{m}_h, \dot{m}_c$	mass flow rates [kg/s]	h	convective heat transfer rate [W/m^{2}K]
C_{pc}, C_{ph}	specific heats [J/kg.K]	Nu	nussalt number [-]
$T_{c,out}, T_{h,out}$	outlet temperatures [°C]	R_e	Reynolds- number [-]
$T_{c,in}, T_{h,in}$	inlet temperatures [°C]	V_{max}	maximum air velocity in tube bank
U	overall heat transfer coefficient [W/m^{2}K]	D_r	root diameter [m]
ΔT_{lm}	log mean temperature difference [-]	ℓ	fin spacing [m]
F	the correction factor of heat transfer rate [-]	b	fin height [m]
R_f''	fouling resistance per surface area [m^{2}K / W]	τ	fin thickness [m]
R_{tot}	total resistance [K/W]	k	thermal conductivity [W/m.K]
R_w	resistance tube wall [K/W]	μ	dynamic viscosity [kg/s.m]
$\dot{Q}_f$	fin heat transfer rate [W]	h_o	Gas-side heat-transfer coefficient [W/m^{2}K]
E	heat exchanger effectiveness [-]	P_T	pitch distance [m]
A_b	area at the base of the fin [m^2]	D_r	root diameter [m]
θ_b	temrature difference between the base and free stream [°C]	V_{face}	face velocity the average air velocity approaching the first row of tubes [m^2]
T_∞	free stream temperature [°C]	P_r	prandtl number, surface roughness term [-]
A_f	the surface area of the fin [m^2]	ρ	density [kg/m^3]
η_f	fin efficiency [%]	ΔP_s	pressure drop for flow across a bank of tubes [Pa]
η_w	overall surface efficiency [%]	ΔP_t	pressure drop for flow in the tubes [Pa]
$\dot{Q}_t$	total heat rate from the surface area A, associated with both the fins and the exposed portion of the base [W]	f	fanning friction factor [-]
G	mass flux [kg/s. m^2]	N_r	number of tube rows [-]
D_f	fin outside diameter [m]	L_2	the core length for flow normal to the tube bank [m]
X_t	pitch in the transverse tube row [m]	A_o	minimum free-flow area [m^2]

X_L	pitch in the longitudinal tube row [m]	**s**	fluid specific gravity [-]
L_1	tube length [m]	**Φ**	viscosity correction factor [-]
L_3	the no flow dimension length [m]		

Subscript

h	hot fluid	∞	free stream
c	cold fluid	**r**	Root
in	Inlet	**max.**	Maximum
out	Outlet	**min.**	Minimum
f	Fin	**t**	in the tube
b	Base	**s**	in the shell

ABBREVIATION

AMASSAS.Co	Awash Melkassa Aluminum Sulfates and Sulfuric Acid Share Company
STHE	Shell and tube heat exchanger
NTU	Number of transfer unit
ACO	Ant colony optimization

BIOGRAPHIES

Melkamu Embiale was born in July in 1993. He received the B.Sc. degree in Mechanical Engineering (Thermal) and the M.Sc. degree in Thermal Engineering from Adama Science and Technology University, Ethiopia, in 2016 and 2019, respectively.

Dr. Addisu Bekele (Corresponding Author) was born in Ethiopia on 10^{th} May 1985. He Completed B.Sc. Degree in Mechanical Engineering in 2004, from Bahir Dar University, Ethiopia, M.Sc. Degree in Mechanical Engineering (Thermal) in 2007 from Addis Ababa University, Ethiopia and PhD Degree in Thermal Engineering in 2012 from Indian Institute of Technology, Roorkee, India. He has published more than 13 articles on international journals, international conferences and national conferences. His research interest areas are renewable energy, fluid flow and heat transfer, numerical and computational analysis, and heat Exchanger.

Dr. Chandraprabu Venkatachalam was born in Tiruchengode, Namakkal (DT), Tamilnadu, India on 25th January 1977, Completed Bachelor of Engineering Mechanical Engineering) in the year of 1999, completed Master of Engineering (Thermal Engineering) in the year of 2005 and completed PhD (Thermal Engineering) in the year of 2014. He has published nine articles in international journal, three articles in international conference and seven articles in national conferences. His research area is heat transfer enhancement in air conditioner using nano fluids and solar energy.

Dr. Mohanram Parthiban, born in Sendamangalam, Namakkal (DT), Tamilnadu, India on 19th June 1978, Completed Bachelor of Engineering (Mechanical Engineering) in the year of 2000, completed Master of Engineering (Thermal Engineering) in the year of 2004 and ompleted PhD (Thermal Engineering) in the year of 2015. He has published four articles in international journal, an article in international conference and two articles in national conferences. His research area is heat transfer, solar energy and thermal energy storage systems.